Geological Survey of Israel
Ministry of National infrastructures
Energy and Water Resources

Seismic hazard assessment in Israel:

Implications for seismicity model and parameters characterizing the regional earthquakes

Tatiana Meirova and Gony Biran

GSI/04/2017 Jerusalem, March 2017

Table of Contents

תקציר **4**

Abstract **4**

1. Introduction 5

2. Database and methodology 10

3. Regional seismicity model 12

3.1 Dead Sea Transform. Brief geological background 12

3.2 Regional b-value based on updated instrumental and historical catalog of GII 13

3.3 Maximum magnitude for Israel region 19

3.4 Dependence of regional seismicity level on slip rate 23

3.5 Impact of regional slip rate on return period 25

4. Seismic parameters of Dead Sea seismogenic zone 26

5. Seismic parameters of Arava seismogenic zone 33

6. Hula – Kineret seismogenic zone 37

7. Summary and conclusions 41

8. The technique for practical evaluation of regional seismicity model 43

References 45

List of Figures

Figure 1. Seismigenic zones defined by Shamir et al (2001), Shapira et al (2007) and regional seismicity compiled from instrumental catalog of Israel. The numeral denotes the No of seismogenic zone. ..7
Figure 2. Selected for analysis seismogenic zones: Arava, Deas Sea Basin and Hula-Kineret. 10
Figure 3. Seismigenic zones and regional earthquakes used for evaluation of regional b-value. 16
Figure 4. Top panel: model of completeness used in calculations of seismic parameters for Dead Sea Transform (model A). Lower panel: Gutenberg – Richter relation for Dead Sea Transform.....17
Figure 5. Top panel: model completeness used in calculations of seismic parameters for Dead Sea Transform (model B). Lower panel: Gutenberg – Richter relation for Israel region.....18
Figure 6. Top panel: model completeness used in calculations of seismic parameters for Dead Sea Transform (model I). Lower panel: Gutenberg – Richter relation for Israel region. 19
Figure 7. $Mmax$ as a function of slip rate for several choices of recurrence times, for three choices of b-value and for two choices of a fault width.....22
Figure 8. Seismicity level as a function of slip rate for three choices of b-value, for two choices of a fault width.....25
Figure 9. Top panel: model of completeness used in calculations of seismic parameters for Dead Sea seismogenic zone (model A). Lower panel: Gutenberg – Richter relation for Dead Sea zone.....28
Figure 10. Top panel: model of completeness used in calculations of seismic parameters for Dead Sea seismogenic zone (model B). Lower panel: Gutenberg – Richter relation for Dead Sea zone.....29
Figure 11. Top panel: model of completeness used in calculations of seismic parameters for Dead Sea seismogenic zone (model C). Lower panel: Gutenberg – Richter relation for Dead Sea zone.....30
Figure 12. Sensitivity of b-value to possible missing historical events. 31
Figure 13. Top panel: model of completeness used in calculations of seismic parameters for Arava seismogenic zone (Model A). Lower panel: Gutenberg – Richter relation for Arava zone.....34
Figure 14. Top panel: model of completeness used in calculations of seismic parameters for seismogenic zone Arava. Lower panel: Gutenberg – Richter relation for Arava zone.. 35
Figure 16. Top panel: model of completeness used in calculations of seismic parameters for Hula – Kineret seismogenic zone (model B). Lower panel: Gutenberg – Richter relation for Hula – Kineret zone..39
Figure 17. Top panel: model of completeness used in calculations of seismic parameters for Hula – Kineret seismogenic zone (model C) . Lower panel: Gutenberg – Richter relation for Hula – Kineret zone.....40
Figure 18. Regional source model proposed in the study.....44

List of Tables

Table 1. Seismicity parameters of seismogenic zones (Shapira and Hofstetter, 2002). Here: Mmin: Minimum magnitude, Mmax: Maximum magnitude, a and b – values (Gutenberg and Richter, 1954) 8
Table 2. Models of completeness threshold for b-value estimation for whole DST 15
Table 3. $Mmax$ as function of slip rate for several choices of b-value (b = 0.96, b = 0.83, b = 76) estimated for recurrence times T1 = 475 y. and T2 = 2475 y. The row with $Mmax$ estimates relevant for regional slip rate of 5 mm/y is indicated by gray color. 21
Table 4. Dependence of seismicity rate A on slip rate estimated for $Mmax = 7.5$ and three choices of b-value. The row with seismicity level estimates appropriate for regional slip rate of 5 mm/y is indicated by gray color....24
Table 5. Return periods of the earthquakes with magnitude equal or greater than threshold magnitude M = 5 estimated for conditions suitable for DST region as a function of slip rate for three choices of b value. $Mmax$ = 7.5. 26
Table 6. The same as in Table 1.5 with threshold magnitude M = 6.5. 26
Table 7. Models of completeness for b-value estimation for Dead Sea seismogenic zone. 27
Table 8. Comparison of seismic moment rate and fault slip rate estimated from observed magnitudes of regional earthquakes (1900-1916 y.) with that obtained from recurrence parameters estimated for Dead Sea seismogenic area 32
Table 9. Models of completeness for b-value estimation for Arava seismogenic zone....36
Table 10. Comparison of seismic moment rate and fault slip rate estimated from observed magnitudes of regional earthquakes and from recurrence parameters obtained for Arava seimogenic area....36
Table 11. Models of completeness for b-value estimation for Hula-Kineret seismogenic zone. 37
Table 12. Seismic moment and fault slip rate estimated from observed magnitudes of regional earthquakes and from recurrence parameters obtained for Hula- Kineret seimogenic zone....41

הערכת סיכונים סיסמיים בישראל:

מודל סיסמי ופרמטרים המאפיינים פעילות סיסמית באזור ישראל

תקציר

מטרת המחקר היא להציג את הפרמטרים המאפיינים את הפעילות הסיסמית באזור ישראל על פי נתונים חדשים. חישובים של הערכים a ו- b נעשו לאזור ישראל כולה, ולשלושה אזורים סיסמוגניים ספציפיים: ים המלח, הערבה וחולה-כנרת.

המודל הסיסמי הנוכחי המְאוּמָץ עבור קוד הבנייה הלאומי IS413 קובע את הפרמטרים של המודל הסיסמי על בסיס הקטלוג האינסטרומנטלי של רעידות אדמה. עם זאת, הפעילות הסיסמית היום מצביעה על קצב הַחלְקה שנתי איטי יותר מאשר ממוצע בטווח ארוך, ולכן המודל הסיסמי הנוכחי אינו שמרני עבור הערכת סיכונים סיסמיים. אנו מציגים את ההשפעה של קצב ההחלקה הנמוך על הפרמטרים במודל הסיסמי. המגניטודה המקסימאלית האזורית, קצב פעילות, וזמן החזרה נבחנו כפונקציה של קצב הַחלְקה עבור מספר אפשרויות של ערך ה-b .

הניתוח שלנו מראה כי השימוש בערך-b קבוע לאזור ישראל כולה, כפי שנעשה בחלקים רבים של ארה"ב, אינו מתאים לכל האזורים הסיסמוגניים בישראל. הניתוח של מומנט סיסמי וקצב החלקה עבור אזור ים המלח ואזורי ערבה מראה כי המודל הסיסמי הנוכחי אינו שמרני, ומעריך בחסר את הסיכון הסיסמי.

מחקר זה חשוב להערכת סיכונים סיסמיים, ולעדכון התקן הישראלי לבניה, ומוצעת בו טכניקה להערכת הפרמטרים המאפיינים פעילות סיסמית באזור ישראל.

Seismic hazard assessment in Israel:

Implications for seismicity model and parameters characterizing the regional earthquakes

Abstract

A general outcome of this study is to portray the best-fit parameters of regional seismicity according to the new available data. The a and b – value calculations are applied to the whole Israel region and for three specific seismogenic zones: Dead Sea, Arava and Hula-Kineret. To estimate recurrence parameters of data sets of variable completeness with time, a maximum-likelihood approach is used.

The current seismicity model accepted for the national Building Code IS413 (Shapira and Hofstetter, 2002) determines the parameters of regional seismicity mainly based on instrumental earthquake's catalog. However, the present-day seismic activity suggests a much slower annual slip rate than long-term average one and therefore, the present-day seismicity model is not conservative for seismic hazard analysis. In this study we show how much the regional seismic model parameters can be affected by the underestimated regional slip rate. The

regional maximal magnitude, earthquake activity rate, and recurrence time are examined as a function of average fault slip rate for several choices of b-value.

Our analysis shows that using the overall constant b-value, as done in many parts of the USA, is not appropriate for the Israel region. The seismic moment and slip rate analysis for the Dead Sea and Arava seismogenic zones indicates that the current seismic model accepted for National Building Code would yield unconservative and even underestimated seismic hazard.

This research is essential for updating the Israeli Code 413 requirement of regional seismicity model and development of a comprehensive hazard assessment, and a technique for practical evaluation of regional seismicity model is proposed.

1. Introduction

The economic and social effects of earthquakes can be reduced only through a comprehensive assessment of seismic hazard and risk. Upgrading of existing buildings and engineering structures, as well as reliable earthquake resistant design of new structures is necessary. In hazard assessment a seismic hazard model is crucial, because it is used to predict the probabilities of earthquake occurrence and hence the expected damage and loss.

The seismic hazard model requires knowledge of regional seismic sources and their associated earthquake recurrence. The study of seismicity and an adequate assessment of seismic hazard are important for the area of Israel, where regions of high seismic hazard that require the implementation of site effect measures occupy about a half of the area of Israel (Gvirtzman and Zaslavsky, 2009). Definition of the seismic sources in a region is the important and critical inputs for seismic hazard assessment. In each seismogenic zone it is presumed that seismicity has a homogeneous character, such that earthquakes have an equal probability of occurring at any point in the zone. The definition and characterization of seismic source zones depends on the interpretation of the available geological, geophysical, paleo seismic information and seismological data obtained by many tools such as tectonic studies, seismicity, surface geological investigations and subsurface geophysical techniques. Each zone is defined according to following parameters:

1) Geometry (defined by spatial distribution of regional earthquakes)

2) The magnitude-frequency parameters of the seismicity

3) The maximum magnitude

4) The depth distribution

5) The expected orientations of faulting

The seismogenic zones in the region of Israel were identified by Shamir et. al., (2001), approved in 2007 with minor changes (Shapira et al., 2007) and accepted as the basis of national Building Code IS413. Figure 1 shows the unified seismogenic source model for the Israel region, which consists of a total of 27 sources and regional seismicity available from the GII instrumental and historical earthquake catalog.

Generally, the seismicity of the region can be described by model of seismicity defined by the Gutenberg – Richter (1954) relation. It is assumed that earthquakes on each fault occur according to the formula:

$$\log(N) = a - bM \qquad (1)$$

where M is magnitude, a and b are constants and N is number of earthquakes equal to or larger than M.

In addition to the Gutenberg – Richter model alternative models of seismicity exist, such as double exponential (Lomnitz-Adler and Lomnitz, 1979), or one following from the Kulbak principle of maximum entropy (Main and Burton, 1984; Kagan, 1991, 1994). A fundamental importance for the seismic hazard assessment is the tail behavior of the distribution of strong earthquakes. Short instrumental earthquake catalog and a large error in determining the magnitude of paleo-earthquakes do not allow to reliably investigate the distribution of regional earthquakes on the basis of empirical data. Earthquake occurrence is typically more complicated than the models on which hazard calculations are based, and the available history of seismicity is almost always too short to reliably establish the spatiotemporal pattern of large earthquake occurrence. The earthquake recurrence in Israel region is variable and still not well understood. For PSHA calculations in Israel the model of seismicity defined by the Gutenberg – Richter relation is commonly accepted. Therefore the estimation of b-value and its uncertainty is crucial for seismic hazard studies, as well as verifying theoretical assertions, such as, for example, the universality of the Gutenberg-Richter relation.

In the relation (1) a-value is concerned with regional seismicity level, and is related to the number of events and period of time. The b-value reflects the relative proportion of the number of large to small earthquakes in the region, and is related to the stress condition over the region. The b-value is considered to be closely related to tectonic characteristics of a region (Hatzidimitriou et al., 1985; Wang, 1988; Tsapanos, 1990). It seems to be in close connection with the geological age of an area (Allen et al., 1965). Tsapanos (1990) found significantly different b -values in east and west Pacific and suggested that this is related to the difference in the mechanical structure of the material in each area, as well as to their tectonic evolution. Manakou and Tsapanos (2000) suggested that low b -values are related to low degree of heterogeneity, large strain rate, large velocity of deformation and therefore large fault. On the other hand there are evidences (Yılmazurk et al., 1999; Bayrak et al., 2002) that a and b -values do not always supply much information about the tectonics of an area.

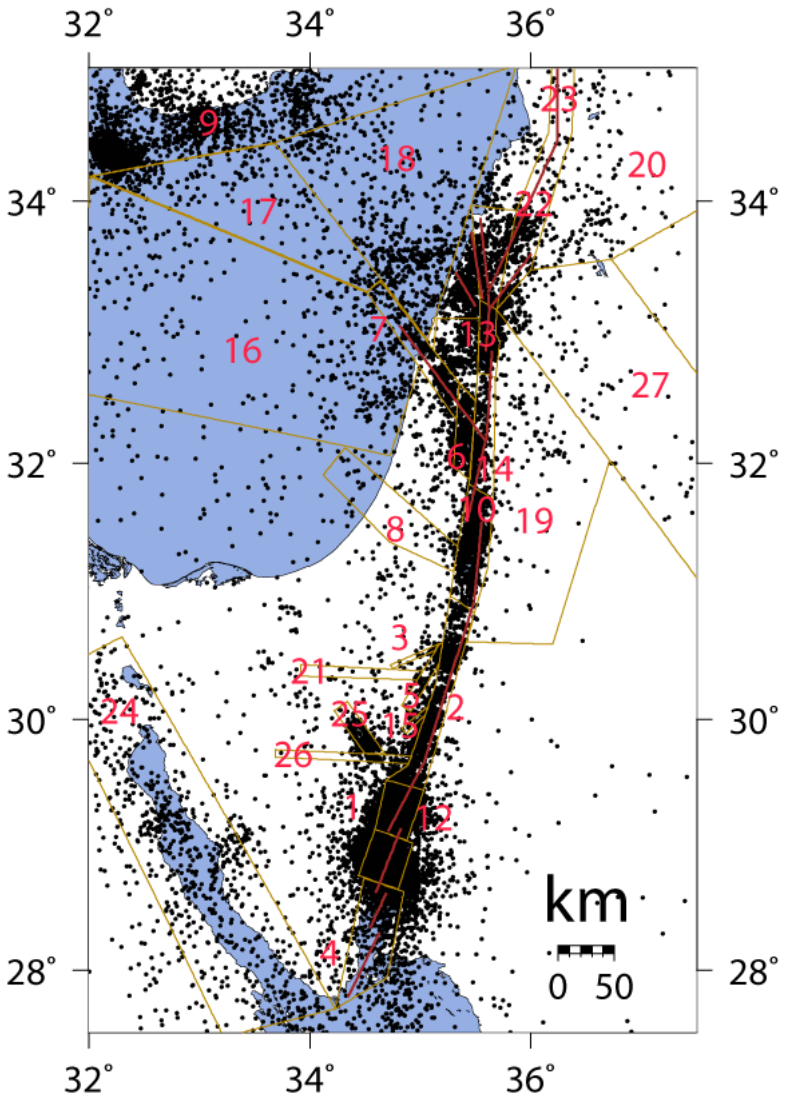

Figure 1. Seismigenic zones defined by Shamir et al (2001), Shapira et al (2007) and regional seismicity compiled from instrumental catalog of Israel. The numeral denotes the No of seismogenic zone.

For most seismically active regions on Earth, the b-value is normally close to 1.0 but varies between 0.5 and 1.5 (Pacheco et al., 1992; Wiemer and Wyss, 1997). It is observed that b-value varies with time and prior to the occurrence of a large shock (e.g. Imoto, 1991; Jaumé and Sykes, 1999). Many factors can cause perturbation of the normal b-value. According to Wyss (1973), an area with low b-value is considered to have increased stress, i.e the area is considered as high potential of future large shock. Nuannin et al. (2005) have observed that the area around the epicenters of the Sumatra earthquakes of 2004, Mw9.0 and Mw8.7 of 2005 occurred within the zones of low b-values. Main et al. (1989) have shown that during the earthquake cycle b-value varies between 0.5 and 1.5, and regions with b=0.5 are in a state of critical failure, in risk of experiencing a large earthquake. Many studies show that data of good quality and quantity provide temporal and spatial distribution of b-value. Recently, Roy et al. (2012) have observed that the lower b-value structures are the source zones for the great

earthquakes of Mw>7.5 in the Andaman-Sumatra Subduction Zone. Several researchers have shown variations of the b-value depending on the depth of earthquakes source (Popandopoulos and Chatziioannou, 2014). However, some scientists believe that b-value is constant showing that the temporal and spatial distribution of b-value are effected by statistical or data errors (Abercrombie and Brune, 1994). In Israel for PSHA calculations the seismicity parameters quantified by Shapira and Hofstetter, (2002) are adopted and accepted by the national Building Code IS413. Each of seismogenic zones is characterized by the corresponding seismicity parameters in terms of minimum and maximum magnitude, and earthquake occurrence rates. The parameters for seismogenic zones are given in Table 1.

Table 1. Seismicity parameters of seismogenic zones (Shapira and Hofstetter, 2002). Here: Mmin: Minimum magnitude, Mmax: Maximum magnitude, a and b – values (Gutenberg and Richter, 1954)

No	Name	Mmin	Mmax	a	b
1	Aragonese	4.0	7.5	2.27	0.96
2	Arava	4.0	7.5	2.26	0.96
3	Arif	3.8	5.5	1.635	0.96
4	Arnona-Dakar	4.0	7.5	2.52	0.96
5	Barak	3.8	5.5	1.724	0.96
6	Beit Shean-Gilboa	4.0	6.5	2.17	0.96
7	Carmel	4.0	6.5	2.17	0.96
8	Central-Israel	3.5	5.5	1.53	0.96
9	Cyprus	4.0	8	3.26	0.96
10	Dead-Sea	4.0	7.5	2.52	0.96
11	Eilat	4.0	7.5	2.27	0.96
12	Galil	3.8	5.5	1.2	0.96
13	Hula-Kineret	4.0	7.5	2.3	0.96
14	Jordan-Valley	4.0	7.5	2.52	0.96
15	Malhan	3.5	5.5	1.37	0.96
16	Mediterranean-1	4.0	6.5	2.785	0.96
17	Mediterranean-2	4.0	6.5	2.785	0.96
18	Mediterranean-3	4.0	6.5	2.785	0.96
19	North-Jordan	4.0	5.5	2.205	0.96
20	Palmira	4.0	6	2.262	0.96
21	Paran	3.7	6.0	1.995	0.96
22	Roum	4.0	7.5	2.42	0.96
23	Yamune	4.0	7.75	2.966	0.96
24	Suez	4.0	7	3.03	1.07
25	East-Sinai	3.8	6.0	1.67	0.96
26	Thamad	4.0	6	1.955	0.96
27	W.-Sirhan	4.0	6	2.37	0.96

The present seismicity model for Israel region suggests a constant b-value for the entire region as is done in the USA. Shapira and Hofstetter (2002) determined the b-value using a maximum likelihood method for the time period of 1900 through 2000 (a total of 100 years) as 0.96. In previous studies Salamon et al. (1996) obtained b value of 1.00 for the whole Dead Sea Transform for a 95 year period; Arieh (1967) estimated a b-value as 0.8 for a 60 year period; Ben-Menahem and Aboodi (1971) obtained b-value of 0.86 for a 2,500 year period; Shapira and Feldman (1987) got it as 0.8 for a 10 month period and Hamiel et al., (2009) for several segments of DST found b =0.95 based on historical data.

Hazard assessments are indirectly proportional to the slip rate (Youngs and Coppersmith, 1985). Seismic moment release on a fault is proportional to the average slip on the fault during the earthquake, and the sum of the moments of all the earthquakes on a fault is proportional to the total seismic slip of the fault (e.g., Brune, 1968, etc). Therefore, if all the slip which accumulates because of plate tectonic motion is relieved in earthquakes, then the slip rate on the fault is directly related to the seismicity on that fault. In Israel and in neighboring areas, geologically estimated deformation rates are overall very low, consistent with recent GPS measurements. Ongoing investigations of the regional slip rate along the Dead Sea fault, such as the geological analysis (Garfunkel et al, 1981) and GPS measurements (Sadeh et al, 2012) show that regional slip rate vary between 0.5 and 10 mm per year and is changed along different segments of DST. The average total slip rate between Africa and Arabia is commonly justified as 5 mm per year and is consistent with long-term geological strain rates. However, the present-day seismic activity suggests a much slower annual slip than long-term average one. Salamon et al. (2003) estimated the seismic moment release during the previous century as 40 per cent of the expected energy release from regional seismicity.

Following Gargunkel et al. (1981) and Ben-Menahem et al. (1976) the possible reasons for such observation might be such as:

1. In the DST region an unusually large fraction of the total motion takes place by non-seismic creep.
2. Earthquake of magnitude 8-8.5 which generates moments of 3×10^{28} dyne - cm and can contribute a slip of 0.33 cm/y has occurred once in last 4000 y.
3. During the last 1000-10000 y the slip rate was actually slower than the long-term average. This is compatible with the locally discontinuous expression of the strike-slip faults in the Lisan beds, and especially with the absence of notable systematic offsets of all post-Lisan streams in the Jordan Valley.

Shapira and Hofstetter (2002) determined the parameters of regional seismicity mainly based on instrumental catalog. They note that their estimates are consistent with average regional slip rate of 2 mm/y and not consistent with long-term slip rate. Therefore, the present-day seismicity model is not conservative for PSHA, i.e., suggested seismicity parameters are the upper bounds to the present-day regional seismicity. In this study we show how much the regional G-R seismic parameters such as maximum magnitude, rate of regional seismicity and return period can be biased by the underestimated regional slip rate.

The purpose of this study is to revise the parameters characterizing regional seismicity on the basis of new seismological data. We also consider the question how much regional seismic parameters can be biased by the underestimated regional slip rate. To demonstrate the limits of regional seismic parameter's estimates we analyze three representative sections of the DST:

Arava, Dead Sea basin and Hula- Kineret zone. Figure 2 shows the selected zones with analyzed earthquakes extracted from instrumental and historical catalogs. For specified fault areas the moment and slip rate analysis is performed by comparison of the observed rates with theoretical one that are based on different recurrence relationships.

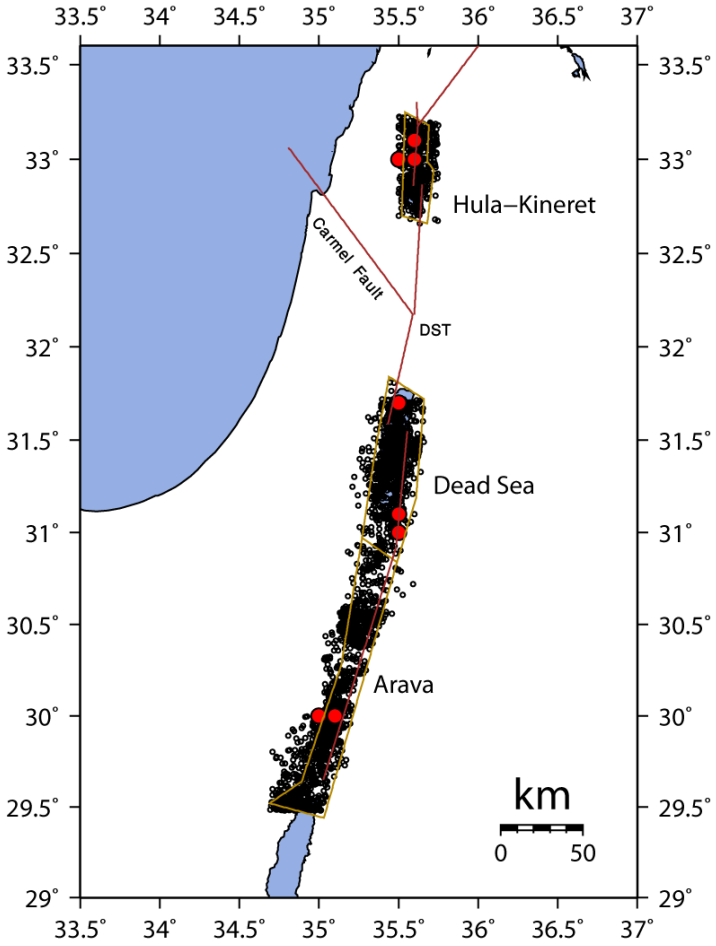

Figure 2. Selected for analysis seismogenic zones: Arava, Deas Sea Basin and Hula-Kineret. The open black circles indicate the earthquakes relevant for analysis of b-value estimates extracted from GII instrumental catalog. Red circles show the distribution of historical earthquakes used in analysis. Brown line schematically shows the DST and Carmel fault.

2. Database and methodology

The database for this study is the updated catalog of local and regional earthquakes up to January 2016 available from the Israel Seismic Network operating under supervision of Geophysical Institute of Israel. To model the occurrence parameters, the historical catalog of moderate-to-large earthquakes is used, along with the instrumental one. The resulting earthquake catalog for selected zones integrates information from different sources:

- The epicenter locations of the ISN (GII) with events since 1900.

• Information from the historical earthquake catalog of Israel and neighboring countries (GII).

The historical cataloq covers the time span from 1200 B.C. to 1900, and is compiled by analysts of GII from the published bulletins of Amiran et al, (1994), Ambraseys (2001), Jordan Seismological Observatory, etc.

For the purposes of the present study we use moment magnitude which better (when compared with body-wave or surface-wave magnitude) indicate the size of earthquakes. M_w gives a magnitude estimate directly related to seismic moment without saturation for great earthquakes and being comparable to other magnitude. Duration magnitudes are converted to the moment magnitudes M_w using a formula from Hofstetter and Ataev (2011) based on a large data set of regional earthquakes:

$$M_w = 0.9\ M_d + 0.11 \qquad (2)$$

For b-value computation two methods are commonly used: the least-squares and the maximum-likelihood method (Weichert, 1980). The reliability of these methods depends upon many elements: the sample size, the errors in data, the choice of binning magnitudes, and the difference between the threshold magnitude and the maximum possible magnitude considered for the region examined. However, the maximum-likelihood method is generally considered statistically more efficient and less dependent upon the few events observed in high magnitude bands. The use of the least squares technique does not have any statistical foundation (e.g., Page, 1968; Bender, 1983).

We apply the maximum likelihood methodology allowing the calculating the b-values using the different magnitude completeness levels for various time periods. In the method the b-value is defined by the relation:

$$\frac{1}{\beta} = \bar{M} - M_0 - \frac{Mexp\big(-\beta(M - M_0)\big)}{1 - exp\big(-\beta(M - M_0)\big)} \qquad (3)$$

where $\beta = b\ ln(10)$, $\bar{M}$ is the average magnitude of the sample, M_0 is the minimal magnitude at which event observations are considered complete (Weichert, 1980). The standard error of the maximum-likelihood estimation of b is approximately $b/\sqrt{N}$, for large N (the number of earthquakes with, $M \geq M_0$). b follows the $\chi 2$ statistical distribution and the statistical significance of the difference in the b -value, for two different earthquake groups, can be tested by the F-distribution (Utsu, 1966).

Seismicity statistics are related to the rate of slip along a given fault from earthquakes, using the concept of seismic moment. Campbell (1977), Anderson (1979), Molnar (1979), Papastamatiou (1980) have all proposed a number of functional forms of the occurrence relation so that the seismicity is consistent with the known crustal deformation rates. We select the particular functional form of the truncated occurrence relation from the many which were proposed. For illustration of sensitivity for recurrence parameters of regional seismicity mainly regarding value of slip rate we selected the relation (2) in Anderson and Luco (1983).

$$N(M) = A\left[\left(e^{\bar{b}\,\Delta M} - 1\right) + B\ \bar{b}\Delta M + C\right] H\ \Delta M \qquad (4)$$

where H is the Heaviside step function, $\Delta M = M_{max} - M$, $\bar{b} = \ln b$. We use this functional form by setting $A = 10^{a-bMmax}$; B=0; C=1. This form is widely used in probabilistic seismic hazard studies. This constrain defines the cumulative occurrence rate of earthquakes with magnitude greater than M as an exponential function truncated at M_{max}. The link between slip rate and earthquake recurrence rate is made through the seismic moment:

$$\mu\, A\, S = \frac{bN(M_{max})M_0(M_{max})\exp\big(-\beta(M_{max}-M)\big)}{(c-b)\big(1-\exp\big(-\beta(M_{max}-M)\big)\big)} \qquad (5)$$

Finally, we compare seismic moment rate estimated from fault slip rates in a region with seismic moment rate based on seismicity data. For doing this we will use the Hanks and Kanamori (1979) definition of seismic moment through the moment magnitude.

$$\log M_0 = cM_w + d \qquad (6)$$

where c = 1.5, d = 16.1. (dyne*cm)

3. Regional seismicity model

3.1 Dead Sea Transform. Brief geological background

The DST, stretching from the Red Sea to the Tauros-Zagros collision zone, is a conspicuous active shear zone that forms the plate boundary between the Sinai microplate in the west and the Arabian Plate in the east. The length of the DST exceeds 1000 km. It extends from the Gulf of Eilat in the south through the Wadi Araba, the Dead Sea basin, and continues northward through Yammouneh fault that intersects with the Arabia-Eurasia collision zone in southern Turkey. The formation of the transform fault started in the Early Miocene (at approximately 17 Ma) and led to a total left-lateral displacement of 105 km until today (Freund et al. 1970; Garfunkel 1981). On the basis of geological, geodetical (GPS), and paleoseismological techniques, it was shown that the slip rate varies between 0.5 and 10 mm/yr through time (Garfunkel et al. 1981; Klinger et al. 2000a; Pe'eri 2002). Recent studies (Wdowinski et al. 2004; Le Beon et al. 2008; Sadeh et al. 2012) reported somewhat smaller slip rate values from 3.1 to 5.4 in various parts of the Dead Sea Transform. Garfunkel et al. (1981) propose possible variation of slip rate over periods of a few 1000 y.. Hamiel et. al (2009) suggest a stable mode in the seismicity of the Dead Sea Transform during the past 60,000 yr.

The internal structure of the DST is dominated by left-lateral en-echelon strike-slip faults (Garfunkel et al. 1981). These en-echelon faults have produced several pull-apart rhomb-shaped grabens that have formed deep basins. The largest of these are the Dead Sea basin and the basins that make up the Gulf of Eilat (Ben-Avraham 1985). The pull-apart basins are bordered by extensions of major strike-slip faults (Garfunkel and Ben-Avraham 1996). The average depths on the transform faults are of ~ 15 km with a standard deviation of 3.0 km (Hofstetter et al, 2013).

3.2 Regional b-value based on updated instrumental and historical catalog of GII

Initially, we assess the overall b-value for the entire Israel region. In regional hazard studies, an overall b-value is often used in order to stabilize the result by avoiding undue fluctuations of b-value particularly in zones of low seismicity (Frankel, 1995; Frankel et al., 1997b**).**

As it is well known from previous studies there is a significant uncertainty in the assessment of seismic parameters. The main sources of uncertainty in the estimates of a and b values : incompleteness and limited history of the earthquake catalog, the variety of magnitude definitions which can only be related empirically, empirical moment-magnitude relations, uncertainty in fault lengths and seismic thickness, the maximum of expected magnitude and how the recurrence relation is truncated at maximum magnitude.

The level of uncertainty in seismic parameters is very sensitive to completeness of catalog. The catalog completeness for the period 1900–2000 was studied by Shapira and Hofstetter (2002) taking into account the local and regional seismic earthquakes which occurred in the twentieth century and the increasing number of seismic stations in Israel, Jordan and neighbouring countries. Through this period of time the detectability of seismic events has been improved and catalog completeness is considered in the following time steps: $M_d \geq 5.0$ from 1900 to 1939, $M_d \geq 4.0$ from 1940 to 1962, $M_d \geq 3.0$ from 1963 to 1982, and $M_d \geq 2.0$ from 1983 to recent times. The detectability of earthquakes in the Dead Sea Transform is rather uniform since 1983, due to the joint operation of seismological networks of Israel and Jordan (Hofstetter et al, 2013). We revise magnitudes of completeness below.

One of the uncertainty sources is the variety of magnitude types and magnitude relationships which can be related empirically. The GII earthquake catalog lists the magnitudes referred to as the duration magnitudes since 1900. Till 2007 the catalog magnitudes are reported as local magnitudes, but essentially are the duration magnitudes. The duration magnitude estimates suffer from a bias in computed earthquake epicenters caused by the non-uniform distribution of monitoring seismic stations, located on the one (western) side of the DST, as well as the low resolution 1-D velocity model of Israel. As well the epicentral locations of regional earthquakes might be significantly biased by the site effects. The quality of M_d magnitude determination varies spatially for the GII seismograph network that is a subject to changes due to station outages, deactivation and upgrading. Uncertainty of instrumentally determined magnitudes is estimated to be on the order of 0.3 (Meirova et al, 2011).

The errors of macroseismic magnitudes of historical earthquakes based on the conversion from the intensities can be as large as 0.9 magnitude unit and are not always well constrained (Zohar et al, 2016). Uncertainties in magnitude estimates in historical data could cause higher as well as lower threshold magnitudes, so that the characteristics of seismic activity could be erroneous. In addition, it might be mistakes in chronology of historical events. Due to insufficient amount of information relating to earthquakes in Israel region before 1900, the completeness of historical catalog is hard to establish. Completeness of estimates for historical datasets is largely a matter of expert judgment. Zohar et al. (2016) concluded that obvious "holes" in the list of historical earthquakes in Israel region exist. Earthquakes with $M_w < 6$ can certainly be missing from the historical record. As it is shown by Zohar et al, (2016) and

Meghraoui et al. (2003) there is a relatively large number of damaging earthquakes with magnitudes greater than 6 that occurred along the fault over the historical period from 749 AD to 1408 AD. This level of large devastating historical earthquakes contrasts with only a few large earthquakes during the past 6 centuries. We note that change in activity rate in time might cause a complication when estimating recurrence rates. If we ignore the fact that the two periods might have different activity rates, or a-values, and assume a stable activity rate in DST region during the past 60,000 yr, as suggested by Hamiel et al. (2009), then a systematic bias towards a lower b-value will be introduced.

In the hazard studies it is required that the seismicity behaves in a time-independent mode (Giardini, 1999; Frankel, 1995). Time-independent part of seismicity has a Poissonian background distribution while the time dependent part is influenced by interaction between events and may not be representative of the average behavior of a crustal volume. To avoid time-dependent data, the catalog has to be de-clustered by deleting all foreshocks, aftershocks and swarm type activity. A frequently considered type of time-dependent seismicity is earthquake swarms. A swarm, different from typical aftershock-foreshock sequences, contains several earthquakes with about the same maximum magnitude (within 0.3 magnitude units, otherwise, the largest one may be called the mainshock). A swarm can last from minutes to years. Time-dependent seismicity is much more prominent in shallow crustal environments and can consist of more than 40% of all earthquakes.

First of all, to assess the overall b-value for Israel region we correct the instrumental catalog. As a first test, we check the Poisson distribution of earthquakes in instrumental catalog by applying the $\chi 2$-test. Null hypothesis declaring that the distribution of magnitudes in catalog is Poisson was rejected at significance level of 99%. That means that the dataset has to be de-clustered.

It is commonly suggested that b-value relates to a regional tectonic regime. Regional seismicity in Israel is mostly associated with the Dead Sea Transform. We emphasize that the Gulf of Eilat is a transition zone between the Red Sea (a spreading center) and the Dead Sea Transform with distinct tectonic setting (Ben-Avraham, 1985). This zone is considered as one of the most seismically-active zone in the Middle East. As well, seismicity in this area after main shock of M7.2 on 11 Nov. 1995 obviously has long aftershock-foreshock series. For example, the main shock (M_d =7.2) was followed by 733 aftershocks (M_d >2.8) over a 40-day period. There is no unique way to separate time-dependent earthquakes from background ones. Their physical properties are the same, and no established statistical criterion or definition of what exactly an aftershock or foreshock is exist. There are several algorithms of de-clustering, but it is still problematic to separate the background seismicity from clustered components due to their superposition in time and space. The de-clustered catalog is assumed to be of Poissonian earthquake occurrences. For the reasons listed above we excluded the Eilat and Aragonese zone from the processing. However the process of filtering the original catalog to obtain a Poissonian residual catalog is not unique.

Thereto, we removed from catalog the zones that are distant from seismic network and the catalog for these areas is most probably significantly incomplete. In total, due to various reasons, we removed from catalog the events from Cyprus, Eastern Mediterranean Sea, Egypt, Suez, Arnona, Eilat, Aragonese and Yamouneh zones. The residual catalog is then corrected for clusters, swarms and doublets by deleting the events. For doing this we used a hand procedure with visual identification of aftershocks and foreshocks. The catalogue was analyzed in

chronological order. The approach of Gardner and Knopoff (1974) was used which simply defines a space and time window after each event. The parameters of the space - time window are assumed universal for the entire region and study period, and are only dependent on magnitude. Figure 3 shows the seismogenic zones and regional events used for evaluation of regional b-value.

To assess the overall regional b-value for Israel we tested the corrected catalog and a few models of completeness. In order to understand variability of b-value depending on catalog completeness we select 3 models based on Shapira and Hofstetter (2002) and Hofstetter et al, (2013). Table 2 lists the input models for estimation of regional b-value. The last row in the table marked by gray color shows the resulting regional b-value. The models are considering that the data is complete for different periods at different magnitude ranges. Models A and B use the instrumental and historical catalog. Model I contains data from instrumental catalog only. The simple plot of magnitude as a function of time gives an overview of catalog completeness. Visual inspection of frequency-magnitude plot and repeated calculations of recurrence parameters provide additional insight. Visual inspection of Figures 4-6 reveals that magnitudes of completeness obtained in previous studies are properly defined and agree with our corrected catalog. (It should be reminded that magnitude of completeness is the magnitude where the frequency–magnitude curve starts to deviate from a linear trend).

The models A and B that include historical earthquakes are tested, and it is found that for period 1200 – 1700 year over predicted number of earthquakes with magnitude $M_w \geq 6$ is quite significant. Model A predicts 13 events with $M_w \geq 6$ while the catalog includes 12 events for analyzed period. In model B the completeness period for $M_w \geq 6$ the historical record amounts to 33 events. The average number of events per 816 years given by the model B is 40. It could indicate the missing events with $M_w \geq 6$ in the period of 1200 – 1700. The discrepancy between observed and predicted number of events might also be attributed to the temporal variations of seismicity in the region. Two models A and B yield regional b value close to 0.8. Model I is based on instrumental catalog and results the b-value of 0.93, that is close to the previous regional b-value estimates by Shapira and Hofstetter (2002) and Hamiel et al. (2009).

Table 2. Models of completeness threshold for b-value estimation for whole DST

Model A		Model B		Model I	
Period	Mw	Period	Mw	Period	Mw
1700-1899	6	1200-1899	6		
1900-1939	5	1900-1939	5	1900-1939	5
1940-1962	4	1940-1962	4	1940-1962	4
1963-1985	3	1963-1985	3	1963-1985	3
1985-2015	2	1985-2015	2	1985-2015	2
b = 0.80 a= 3.31		b = 0.78 a=3.36		b = 0.93 a=3.88	

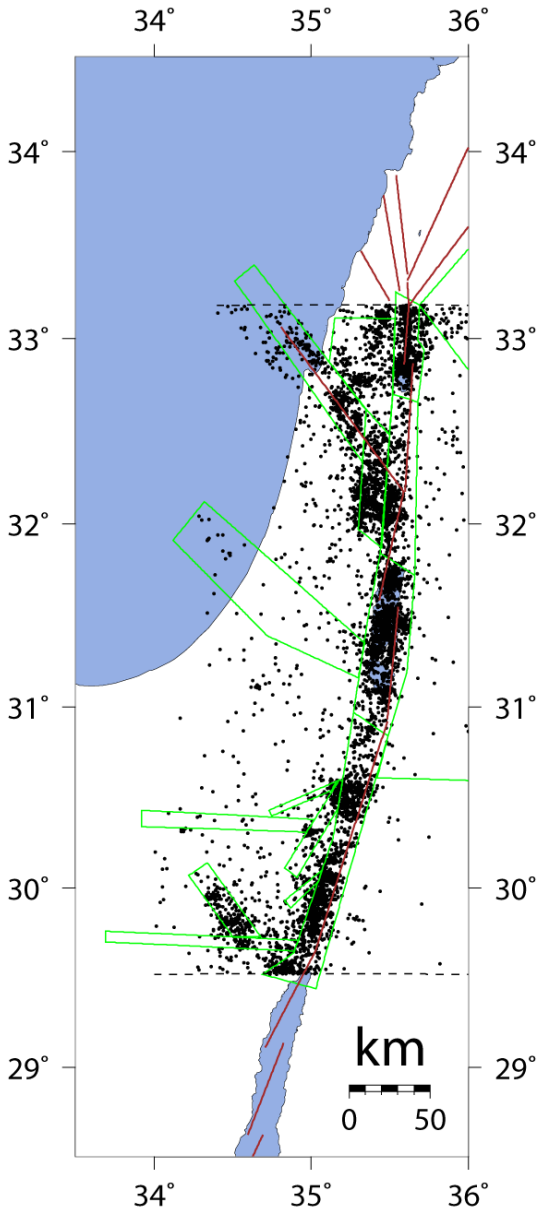

Figure 3. Seismigenic zones and regional earthquakes used for evaluation of regional b-value. The events from zones: Cyprus, Eastern Mediterranean Sea, Egypt, Suez, Arnona, Eilat, Aragonese and Yamouneh are removed. See explanation in the text.

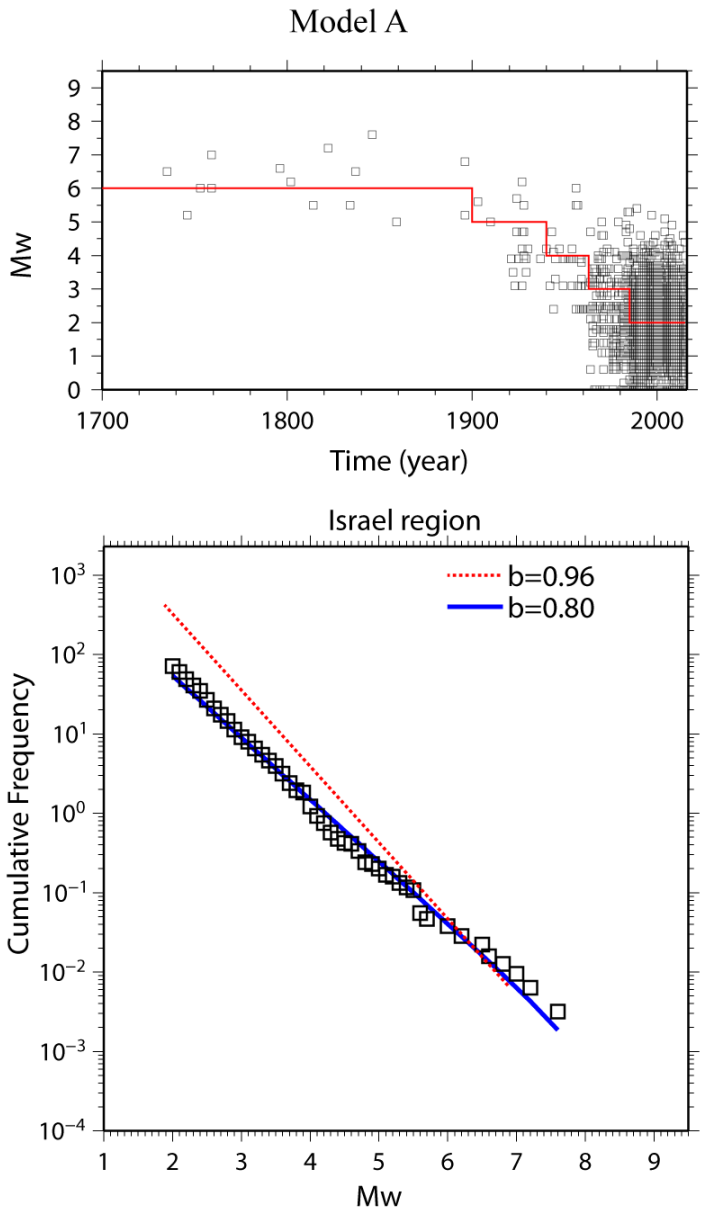

Figure 4. Top panel: model of completeness used in calculations of seismic parameters for Dead Sea Transform (model A). Lower panel: Gutenberg – Richter relation for Dead Sea Transform. Blue solid line with the slop equal to b-value indicates the modeled seismicity line. Open triangles show the observed seismicity. Red dotted line models the seismicity for reference value of b=0.96 that is used in Israel Building Code.

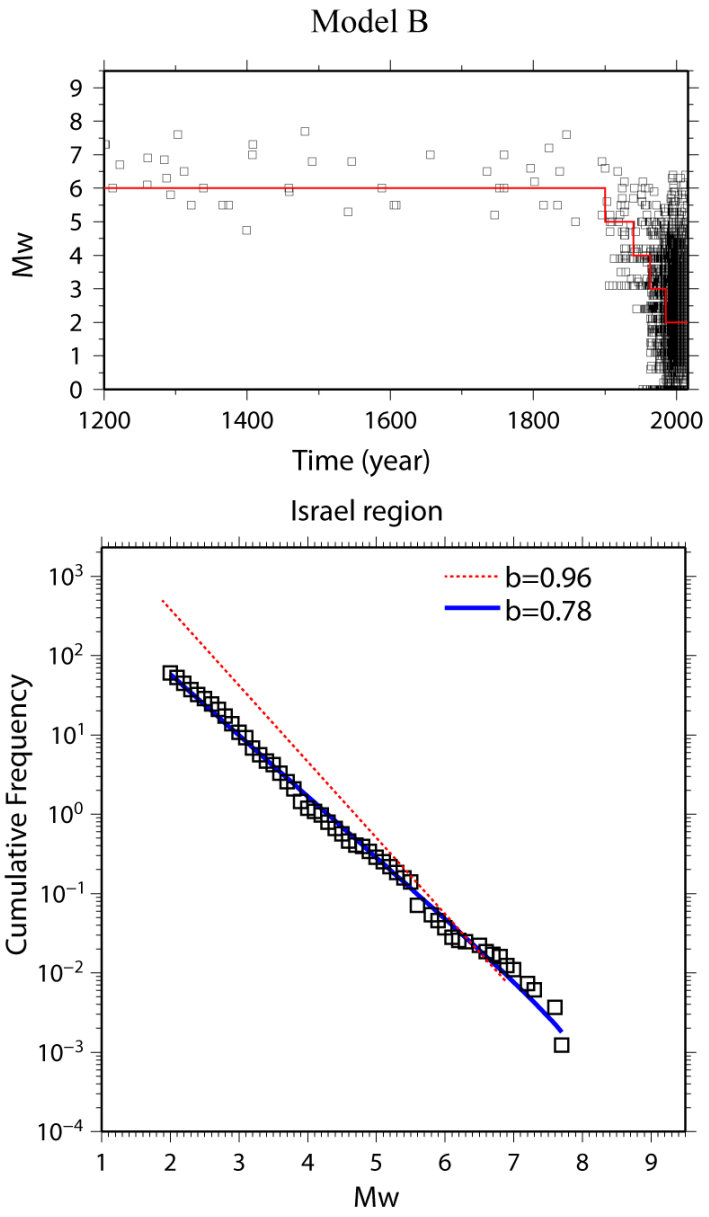

Figure 5. Top panel: model completeness used in calculations of seismic parameters for Dead Sea Transform (model B). Lower panel: Gutenberg – Richter relation for Israel region. Blue solid line with the slop equal to b-value indicates the modeled seismicity line. Open triangles show the observed seismicity. Red dotted line models the seismicity for reference value of b=0.96 that is used in Israeli Building Code 413.

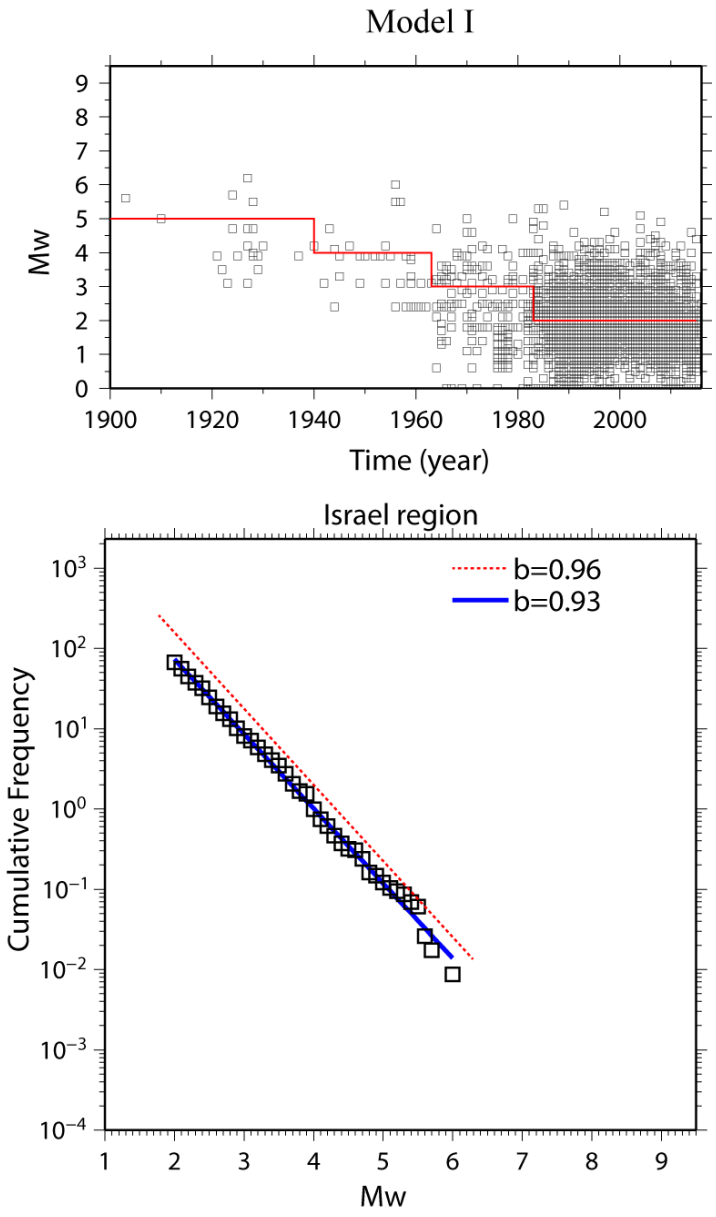

Figure 6. Top panel: model completeness used in calculations of seismic parameters for Dead Sea Transform (model I). Lower panel: Gutenberg – Richter relation for Israel region. Blue solid line with the slop equal to b-value indicates the modeled seismicity line. Open triangles show the observed seismicity. Red dotted line models the seismicity for reference value of b=0.96 that is used in Israeli Building Code 413 without reference to actual a value

3.3 Maximum magnitude for Israel region

The maximum possible earthquake magnitude M_{max} is defined as a parameter with considerable influence on the final hazard at least for long return period. This parameter the most difficult to assess in the study area, because the physical understanding of M_{max} is poor.

This kind of events may have recurrence rates exceeding 10000 years and might not be observable in the historical or geological catalogs.

The slip rate constraints of Anderson and Luco (1983) provide a means to estimate M_{max} from occurrence rates of small magnitude earthquakes. We used this technique in order to demonstrate the limits of M_{max} on slip rate for conditions similar to DST region. We estimate M_{max} for the two known recurrence time (475 and 2475 years) and three choices of b-value (0.96, 0.83, and 0.76). To examine uncertainty introduced by the source depth we calculate variation of M_{max} for $W_1 = 10$ km and $W_2 = 25$ km. Results are shown in Table 3 and Figure 7. In the table the estimates of M_{max} related to the average regional slip rate of 5 mm/year are marked by grey color.

Based mainly on the limited seismic history Shapira and Hofstetter (2001) proposed the maximum magnitude along the DST as 7.5 except the Yamouneh fault with slightly higher magnitude $M_{max} = 7.75$. Our analysis shows that M_{max} defined by Shapira and Hofstetter (2002) for DST region can be underestimated, especially for long periods. Table 3 and Figure 7 demonstrate that for slip rate of 5 mm/y the M_{max} could vary from 7.55 to 8.41. This result is compatible with the assumption of Garfunkel et al, (1981) about the possibility of very strong earthquake (M8-8.5) that could have occurred in the DST in last 4000 y. The existence in the past of even one such strong earthquake can explain the apparent unusually low seismic efficiency of DST.

Table 3. M_{max} as function of slip rate for several choices of b-value (b = 0.96, b = 0.83, b = 76) estimated for recurrence times T1 = 475 y. and T2 = 2475 y. The row with M_{max} estimates relevant for regional slip rate of 5 mm/y is indicated by gray color.

M_{max}						
Slip rate (cm/y)	**b = 0.96**		**b = 0.83**		**b = 0.76**	
	T1	**T2**	**T1**	**T2**	**T1**	**T2**
Fault Width = 10 km						
0.1	7.08	7.56	7.15	7.62	7.18	7.65
0.2	7.28	7.76	7.35	7.83	7.38	7.86
0.3	7.4	7.88	7.46	7.94	7.49	7.97
0.4	7.48	7.96	7.55	8.03	7.58	8.06
0.5	7.55	8.03	7.61	8.09	7.64	8.12
1	7.75	8.23	7.81	8.29	7.84	8.32
15	8.54	9.01	8.6	9.08	8.63	9.11
20	8.62	9.1	8.68	9.16	8.71	9.19
30	8.74	9.21	8.8	9.28	8.83	9.31
100	9.09	9.56	9.15	9.63	9.18	9.66
Fault Width = 25 km						
0.1	7.34	7.82	7.4	7.91	7.47	7.95
0.2	7.54	8.02	7.6	8.11	7.67	8.15
0.3	7.66	8.13	7.72	8.22	7.79	8.27
0.4	7.74	8.22	7.8	8.31	7.87	8.35
0.5	7.8	8.28	7.87	8.37	7.94	8.41
1	8	8.48	8.07	8.57	8.14	8.62
15	8.79	9.27	8.85	9.36	8.92	9.4
20	8.87	9.35	8.94	9.44	9.01	9.48
30	8.99	9.47	9.05	9.56	9.12	9.6
100	9.34	9.82	9.4	9.91	9.47	9.95

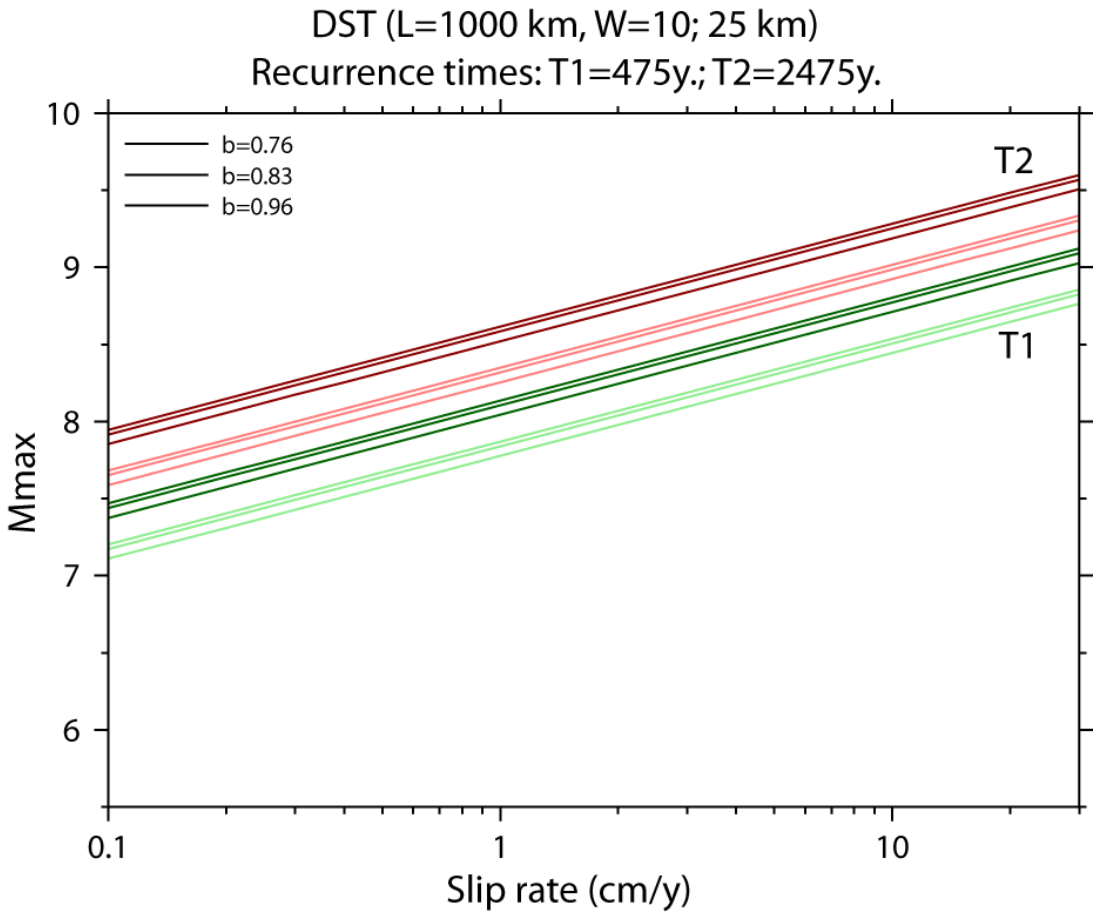

Figure 7. M_{max} as a function of slip rate for several choices of recurrence times $T_1(M_{max}) = 475\ y.$ (dark- and light- green lines); $T_2(M_{max}) = 2475\ y.$ (dark- and light- red lines); for three choices of b-value: 0.96 (bottom line), 0.83(middle line) and 0.76 (upper line) in each troika of lines and for two choices of a fault width $W_1 = 10\ km$ (light green and light red lines) and $W_2 = 25\ km$ (dark green and dark red lines)

Our analysis confirms that M_{max} increases as a slip rate increases and b – value decreases. For the fault where earthquake of M_{max} is occurring once in 475 years the increasing slip rate from 2 mm/y to 5 mm/y will enlarge the M_{max} from 7.28 to 7.55 for a fault area of $\epsilon_1 = 10^4$ km^2(W = 10 km) and from 7.54 to 7.8 for the fault area $\epsilon_2 = 2.5 \times 10^4$ km^2 (W = 25 km). The similar influence of slip rate on M_{max} is observed for return period of 2475 years. Here with, for the slip rate of 5 mm/y that consistent with average regional slip the variation in M_{max} values due to decreasing the b-value from 0.96 to 0.76 is less than 0.15.

We note that difference in our M_{max} estimates reflects the epistemic uncertainty and is dependent on the fault model. The supposed fault width has considerable influence on the M_{max}. Knowledge of actual fault width can considerably reduce the uncertainty in M_{max} estimates.

3.4 Dependence of regional seismicity level on slip rate

If all the slip which accumulates because of plate tectonic motion is relieved in earthquakes, then the slip rate on the fault is directly related to the seismicity on that fault. In order to understand the effect of slip rate on seismicity level we estimate the seismicity rate for conditions appropriate for Dead Sea region.

Relating earthquake rate to slip rate using the recurrence relation requires an estimate of the maximum magnitude for fault. To keep a simplistic model, we use only two different $M_{max} = 7.5$ and $M_{max} = 6.5$. Level of seismicity is estimated for $\alpha = 1.25 \times 10^{-5}$ typical for strike-slip events (Scholz, 1982); $\beta = \sqrt{\alpha\, M_0(0)/\mu W}$. Shear modulus is taken to be ~$3 * 10^{11}$ dyne/crn^2.

Table 4 and Figure 8 show the a comparison of the predicted level of seismicity characteristic for strike-slip faults for three choices of b values (0.96, 0.83, 0.76) and for two choices of a fault width $W_1 = 10\ km$ and $W_2 = 25\ km$. In Figure 8 the seismicity level A related to b=0.96 is indicated by light green, the seismicity level related to b = 0.83 is shown by blue and the seismicity level related to b = 0.76 is indicated by red line. The seismicity level appropriate for the average slip rate of 0.5 mm that commonly accepted as average for DST region is marked by gray color. As it can be seen the rate of seismicity increases with decreasing of b-values and increasing the slip rate and fault width.

Table 4. Dependence of seismicity rate A on slip rate estimated for $M_{max} = 7.5$ and three choices of b-value. The row with seismicity level estimates appropriate for regional slip rate of 5 mm/y is indicated by gray color.

M_{max}	Slip rate (cm/y)	W =10 km			W=2 5 km		
		b=0.96	b=0.83	b=0.76	b=0.96	b=0.83	b=0.76
		A	A	A	A	A	A
7.5	0.10	1.41E-04	1.75E-04	1.94E-04	2.22E-04	2.76E-04	3.06E-04
	0.20	2.81E-04	3.49E-04	3.88E-04	4.44E-04	5.52E-04	6.13E-04
	0.30	4.22E-04	5.24E-04	5.82E-04	6.67E-04	8.28E-04	9.19E-04
	0.40	5.62E-04	6.99E-04	7.76E-04	8.89E-04	1.10E-03	1.23E-03
	0.50	7.03E-04	8.73E-04	9.70E-04	1.11E-03	1.38E-03	1.53E-03
	1.00	1.41E-03	1.75E-03	1.94E-03	2.22E-03	2.76E-03	3.06E-03
	15.00	2.11E-02	2.62E-02	2.91E-02	3.33E-02	4.14E-02	4.60E-02
	20.00	2.81E-02	3.49E-02	3.88E-02	4.44E-02	5.52E-02	6.13E-02
	30.00	4.22E-02	5.24E-02	5.82E-02	6.67E-02	8.28E-02	9.19E-02
	50.00	7.03E-02	8.73E-02	9.70E-02	1.11E-01	1.38E-01	1.53E-01

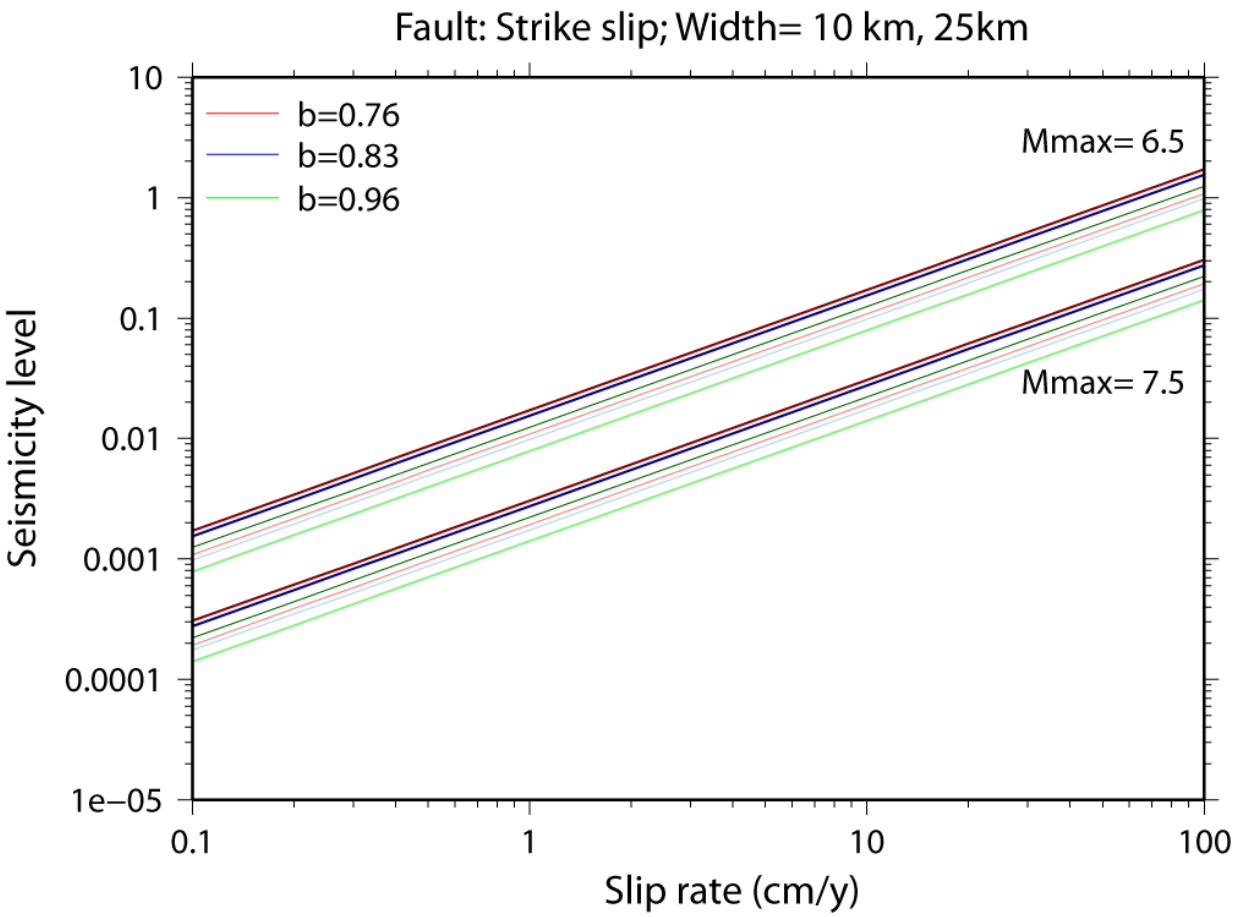

Figure 8. Seismicity level as a function of slip rate for three choices of b-value: 0.96 (green line), 0.83 (blue line) and 0.76 (red line) for two choices of a fault width $W_1 = 10\ km$ (dark green, dark blue and dark red lines) and $W_2 = 25\ km$ (light green, light blue and light red lines). Calculations are performed for $M_{max} = 6.5$ and $M_{max} = 7.5$

3.5 Impact of regional slip rate on return period

In order to understand how much the slip rate affects the return period of the earthquakes with magnitude equal or greater than threshold magnitude we estimated the return period for M_{max} = 7.5 for three choices of b values 0.96, 0.83, 0.76. The predictions are made for threshold magnitudes M = 5 and 6.5 and two different fault width: $W_1 = 10\ km$ and $W_2 = 25\ km$. The results of prediction are listed in table 5 and 6 and shown in Figure 8. It is obvious that return period for earthquakes with magnitude equal or greater than threshold magnitude decrease with increasing fault slip rate. The currently used seismicity model with b=0.96 predicts that the earthquake with M=5 will repeat at least every 6.8 years if slip rate is equal 0.5 cm/y and at least every 3.4 years if a fault slip rate will increase to 1 cm/y. The seismicity model with b=0.76 predicts 5.5 and 2.7 years for similar slip rates. As can be seen from tables 5, 6 the estimates of return time are very sensitive to the fault width.

Table 5. Return periods of the earthquakes with magnitude equal or greater than threshold magnitude M = 5 estimated for conditions suitable for DST region as a function of slip rate for three choices of b value. M_{max} = 7.5.

Slip rate (cm)	W=10 km			W=25 km		
	b=0.96 T (years)	b=0.83 T (years)	b=0.76 T (years)	b=0.96 T (years)	b=0.83 T (years)	b=0.76 T (years)
0.1	33.9	27.3	24.6	17.9	14.4	13.0
0.2	17.0	13.7	12.3	9.0	7.2	6.5
0.3	11.3	9.1	8.2	6.0	4.8	4.3
0.4	8.5	6.8	6.1	4.5	3.6	3.3
0.5	6.8	5.5	4.9	3.6	2.9	2.6
1	3.4	2.7	2.5	1.8	1.4	1.3
15	0.2	0.2	0.2	0.1	0.1	0.1
20	0.2	0.1	0.1	0.1	0.1	0.1
30	0.1	0.1	0.1	0.1	0.0	0.0
50	0.1	0.1	0.1	0.1	0.0	0.0

Table 6**.** The same as in Table 1.5 with threshold magnitude M = 6.5.

Slip rate (cm)	W=10 km			W=25km		
	b=0.96 T (years)	b=0.83 T (years)	b=0.76 T (years)	b=0.96 T (years)	b=0.83 T (years)	b=0.76 T (years)
0.1	2819	2270	2044	1781	1434	1291
0.2	1409	1135	1022	890	717	646
0.3	940	757	681	594	478	430
0.4	705	567	511	445	358	323
0.5	564	454	409	356	287	258
1	282	227	204	178	143	129
15	19	15	14	12	10	9
20	14	11	10	9	7	6
30	9	8	7	6	5	4
50	6	5	4	4	3	3

4.Seismic parameters of Dead Sea seismogenic zone

We now focus on the seismicity model parameters of some seismogenic zones. To model the occurrence parameters in the Dead Sea area the historical catalog of moderate-to-large earthquakes is used, along with instrumental data obtained from the seismic activity along the Dead Sea Transform where the latitude range is from 30.84N to 31.72 N. Throughout the twentieth century, several widely felt earthquakes occurred in 1903, 1928, 1956, 1970, 1979 and 2004, with magnitudes M ~5.0–5.5, causing no or minor damage (Amiran et al. 1994). Five

out of seven relatively moderate-strong events occurred in the Dead Sea basin and two occurred just north of the Dead Sea basin. The strongest recorded event in the last 100 years was the 1927 M6.25 earthquake (Shapira et al., 1993).

Main present-day seismic activity along the Dead Sea Basin is associated with the N-S longitudinal faults, but about the fourth of activity is associated with the east-west trending faults (Ben-Avraham and Schubert, 2006). Seismic activity extends nonuniformly down to depths of 27 km with peak activities at 9–10 km and 15-16 km (Hofstetter, 2012). Length of Dead Sea source zone is approximately 90 km.

Table 7 shows three models of catalogue completeness for Dead Sea zone that are applied for estimation of seismic parameters. The last row in the table shows the resulting a- and b-value. Figures 9, 10 and 11 show the magnitude – frequency curves for the Dead Sea seismogenic zone. Model A produces the b-value equal to 0.78; models B and C yield the b value equal to 0.84 and 0.85, consequently. All models yield a lower b-value than regional b-value estimate.

Table 7. Models of completeness for b-value estimation for Dead Sea seismogenic zone.

Model A		Model B		Model C	
Period	Mw	Period	Mw	Period	Mw
1400-1899	6	1800-1899	6		
1900-1939	5	1900-1939	5	1900-1939	5
1940-1962	4	1940-1962	4	1940-1962	4
1963-1985	3	1963-1985	3	1963-1985	3
1985-2015	2	1985-2015	2	1985-2015	2
b = 0.78 a = 2.51		b = 0.84 a =2.46		b = 0.85 a = 2.47	

It is well known that some earthquakes of less than M6 generally do not produce surface ruptures that contribute to the geological displacement of the ground surface (e.g., Wesnousky, 1986). This occurs when the rupture widths of these earthquakes are less than the width of the fault zone. It implies that some of the historical earthquakes might be missing from the catalog. Anderson and Luco (1983) showed that b-value when measured from events at a single site appears to be smaller than for a fault with specified length. The same effect might be proper for a fault segment. As well some of large earthquakes with magnitude $M < M_{max}$ do not rupture the surface at specific site that make an impression of small b-value. As an illustration of this Figure 15 shows how a number of missed events with different

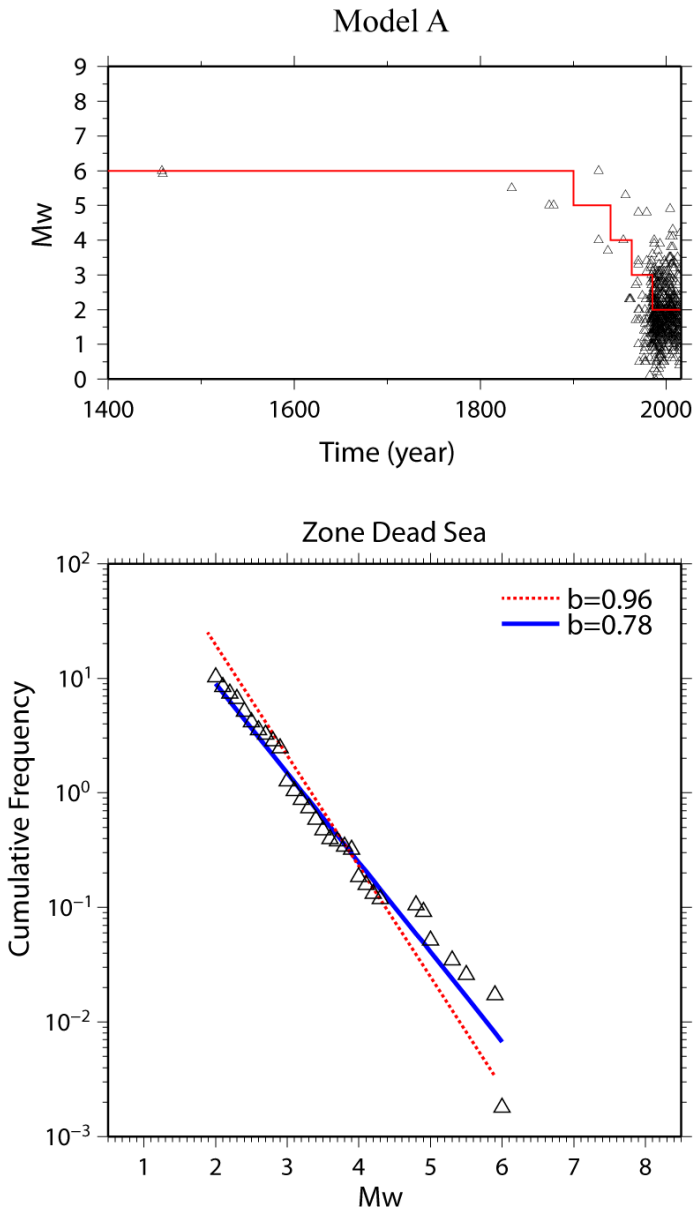

Figure 9. Top panel: model of completeness used in calculations of seismic parameters for Dead Sea seismogenic zone (model A). Lower panel: Gutenberg – Richter relation for Dead Sea zone. Blue solid line with the slop equal to b-value indicates the modeled seismicity line. Open triangles show the observed seismicity. Red dotted line models the seismicity for reference value of b=0.96 that is used in Israel Building Code.

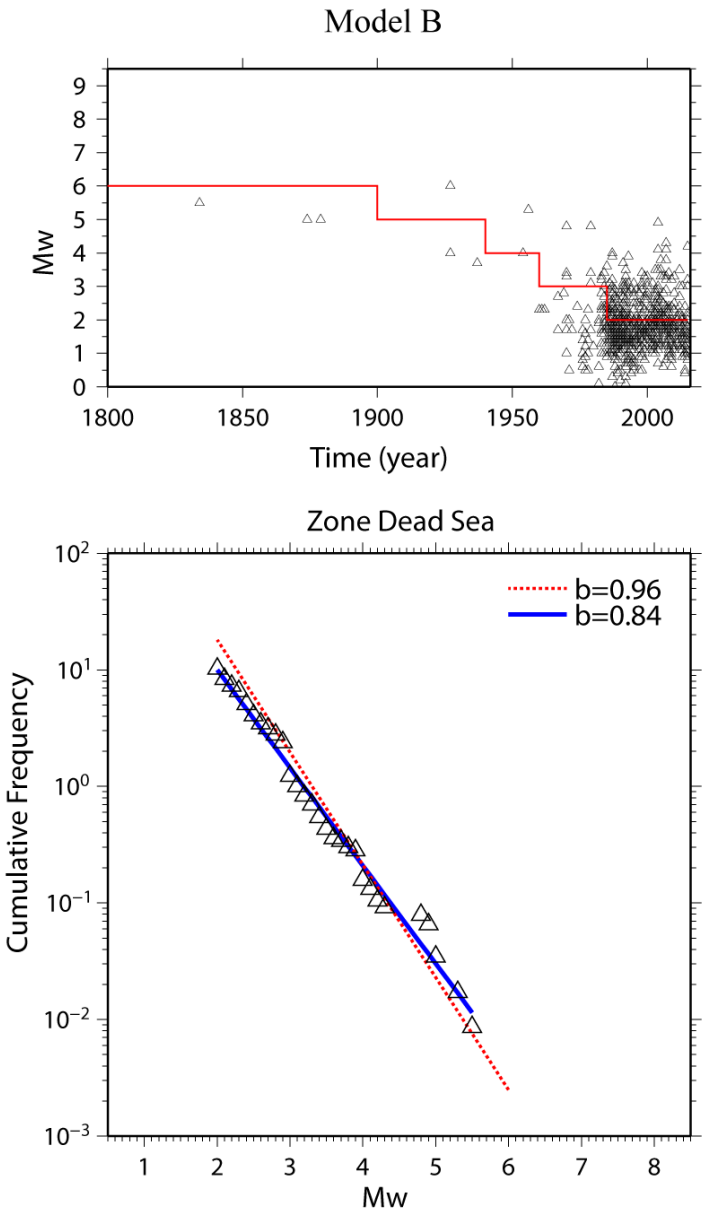

Figure 10. Top panel: model of completeness used in calculations of seismic parameters for Dead Sea seismogenic zone (model B). Lower panel: Gutenberg – Richter relation for Dead Sea zone. Blue solid line with the slop equal to b-value indicates the modeled seismicity line. Open triangles show the observed seismicity. Red dotted line models the seismicity for reference value of b=0.96 that is used in Israel Building Code.

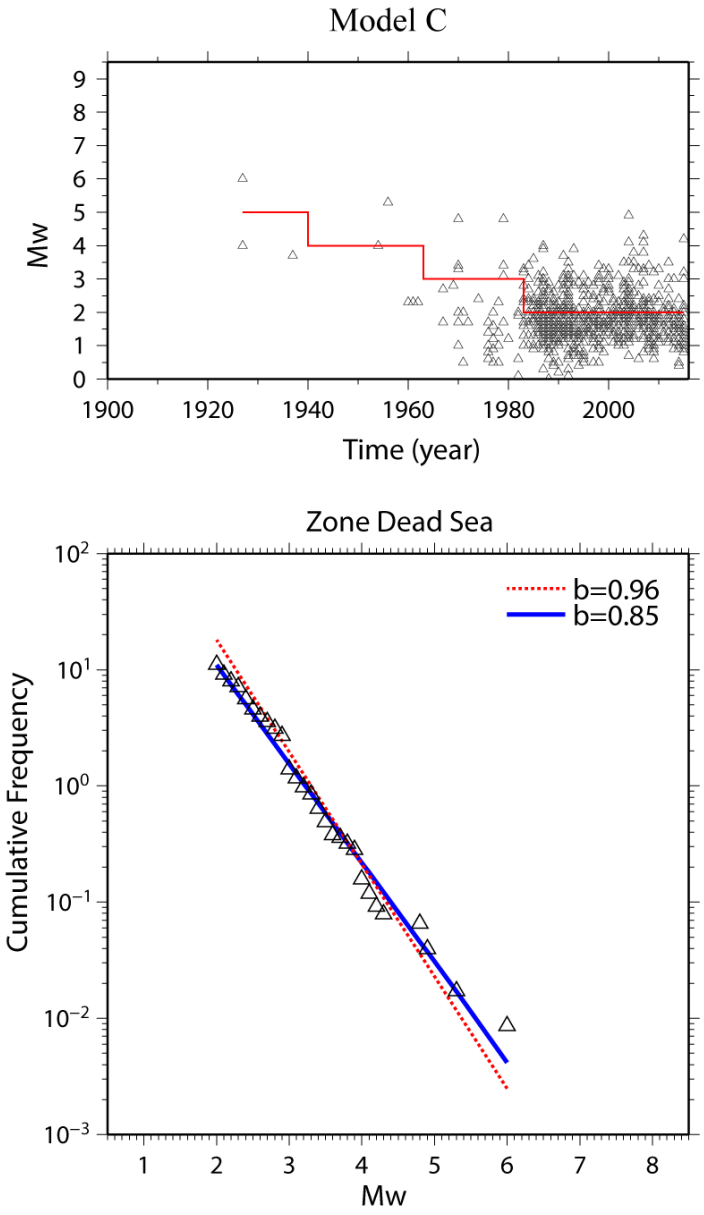

Figure 11. Top panel: model of completeness used in calculations of seismic parameters for Dead Sea seismogenic zone (model C). Lower panel: Gutenberg – Richter relation for Dead Sea zone. Blue solid line with the slop equal to b-value indicates the modeled seismicity line. Open triangles show the observed seismicity. Red dotted line models the seismicity for reference value of b=0.96 that is used in Building Code 413.

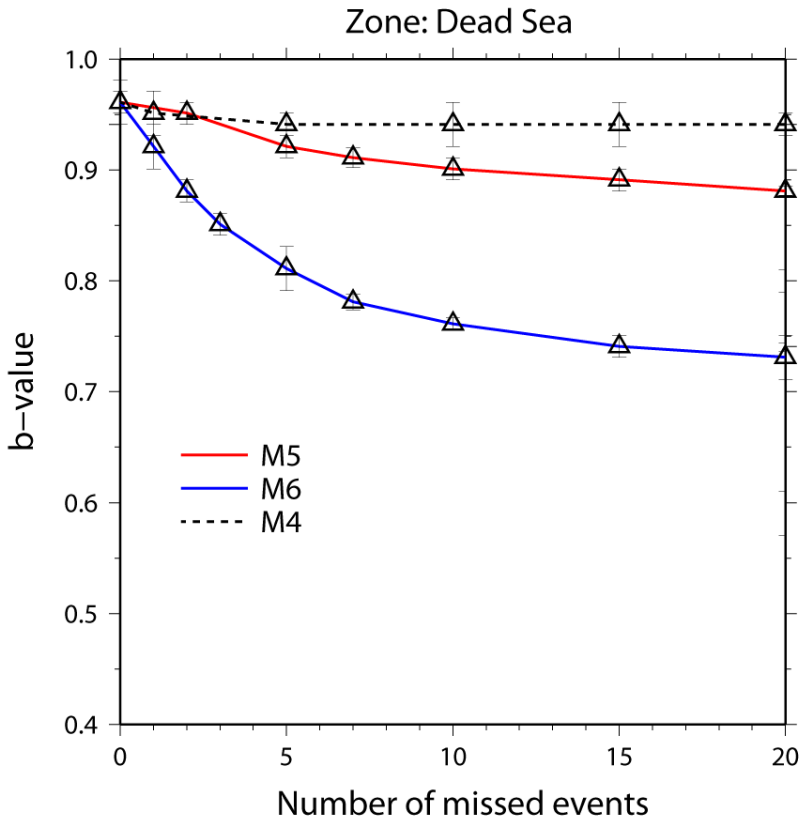

Figure 12. Sensitivity of b-value to possible missing historical events. The blue line indicates the trend of b-value with number of missing events of M6, red line shows the same trend for missing events of M5; dotted line indicates the trend for events with M4. The open triangle shows a b-estimate with error bar.

magnitudes might distort the b-value over the Dead Sea seismogenic zone. With increasing number of missed events b-value decreases. It can be seen that even small number of missed earthquakes with magnitude M≥6 significantly impacts the b-value estimate. It is obvious, that missed earthquakes with magnitude less than magnitude of completeness do not impact the b-value estimates.

From the estimated recurrence parameters we can estimate the seismic moment and then, turn this seismic rate to the rate of fault slip. Table 8 shows the comparison of observed seismic moment rate estimated from magnitudes of regional earthquakes with seismic moment rate based on recurrence parameters. The slip rates obtained from these moments are also shown in Table 8. In the table the row with seismic parameters that used in Israel Building code for PSHA is indicated by gray color. Since the fault width has considerable influence on the slip rate's estimates the comparison is performed for a few different fault width: $W_1 = 5\ km$, $W_2 = 10\ km$, $W_3 = 15\ km$ and $W_4 = 25\ km$. To obtain the observed rate of seismic moment the individual seismic moments from the instrumental catalog for 1900 – 2015 are integrated.

When we compare the slip rate estimated from catalog (S=0.66 mm/y) with that based on the regional a and b values that currently are using in Israel (S=0.18 mm/y), it is certainly to be larger. This observation indicates that selected a and b- values do not agree with present-day regional seismic activity in the Dead Sea area and could underestimate seismic hazard. On the other hand, when we compare the slip rate estimates based on catalog with the accepted measured average slip rate on DST (5 mm/y) it can be seen that slip rate calculated from magnitudes is too small. This observation is in agreement with previous studies (Salamon et al, 2003, Hofstetter and al., 2013) and implicates that much motion does not take place on the DST. One possible explanation for this is that the missing deformation is aseismic and occurs on creeping faults as continuous deformation.

Table 8. Comparison of seismic moment rate and fault slip rate estimated from observed magnitudes of regional earthquakes (1900-1916 y.) with that obtained from recurrence parameters estimated for Dead Sea seismogenic area

Fault width, (km)	**a value (Mw min=2; Mw max=7.5)**	**b-value**	**Mo rate observed (N*m/y)**	**Mo rate (N*m/y) estimated**	**slip rate (mm/y) based on Mo observed**	**slip rate (mm/y) based on recurrence relation**
15	2.52	0.96	2.65E+16	7.41E+15	0.66	0.18
5	2.47	0.85		3.25E+16	1.97	2.41
10					0.98	1.20
15					0.66	0.80
25					0.39	0.48
5	2.51	0.78		9.88E+16	1.97	7.32
10					0.98	3.66
15					0.66	2.44
25					0.39	1.46

One more possible reason for such disagreement is an incompleteness of catalog. Not recorded small magnitude seismic activity can significantly bias estimates of seismic moment amount released on DST, and, consequently, the slip rate estimates.

As it can be seen from table the calculated slip rate is inversely proportional to the seismic fault width if the other parameters are unchanged. The observed slip rate value agrees with slip rate estimate for fault width of 15 km.

The comparison of the observed and estimated seismic moment and fault slip rates indicates that the models of seismicity with b=0.85 and b=0.78 are appropriate for the recorded seismic activity in the Dead Sea seismogenic zone. The slip rate estimated by these models is close to the average fault slip rate and can vary from 0.39 to 7.32 sm/y depending on assumed recurrence model and fault width.

5. Seismic parameters of Arava seismogenic zone

For analysis we selected the regional earthquakes limited by the area between 30.97°N and 29.44 °S (Figure 1, 2). Length of Arava zone is approximately 160 km. In spite of seismic activity extends down to depths of 22 km the peaks of activities are at 5-7 km and 10-14 km (Sadeh et al., 2012).

The Wadi Araba fault is the principal fault strand of the Dead Sea Transform System between the Gulf of Eilat and the Dead Sea. The Wadi Araba fault is outlined by scarps, small rhomb-shaped grabens, pressure ridges and displaced alluvial fan toes indicating that strike–slip faulting is still active and is considered to be the main active strike–slip fault strand of the DST (Garfunkel et al., 1981; Ginat et al., 1998; Klinger et al., 2000; Niemi et al., 2001). The present rate of plate movement as measured by a Global Positioning System (GPS) is assumed as 3.5-6.3 mm per year (Le Beon et al. 2008).

Today's seismicity along the Wadi Araba fault is moderate, and only 25 - 50 smaller magnitude earthquakes occur per year along this segment. Several strong earthquakes hit the region in the last centuries, but with a long cycle (M>6.5 in 1212, M7 in 1168; Marco et al., 1996; Zohar et al, 2016). Shapira and Hofstetter (2001) found very low seismicity level in Arava seismogenic zone over the instrumental period and obtained an unacceptably high b-value close to 2. They argue that lack of seismic activity in the fault area implies the existence of a seismic gap in recordings that could imply the incompleteness of historical catalogs or the accumulation of seismic energy in this region. We note that high b-value can be caused by earthquake series with low stress produced by structural anomalies in the crust (Scholz, 1968; Wyss, 1973). Often large departure from b = 1 to the larger b-values occurs when the seismic activity is presented by swarms (i.e. in swarms no or fewer large earthquakes accompany the occurrence of small magnitude events). Laboratory tests (Warren and Latham, 1970) show that an increase of thermal gradients may cause an increase of b value to 2.7. However, all these reasons may indicate an underestimation of seismicity level in Arava zone and consequently, following underestimation of seismic hazard in the area.

For estimation of seismic parameters for Arava zone we applied two models of catalogue completeness. Table 9 shows these models. Lower row in the table demonstrates the resulting estimates of a and b-values for Arava sesismic zone. For both two models we could not find high b-values, as it was previously established by Shapira and Hofstetter (2001). Figures 13 and 14 show the frequency-magnitude distribution of earthquakes for Arava seismogenic zone. In the figures the blue line represents the best MLE fitting model to the data.

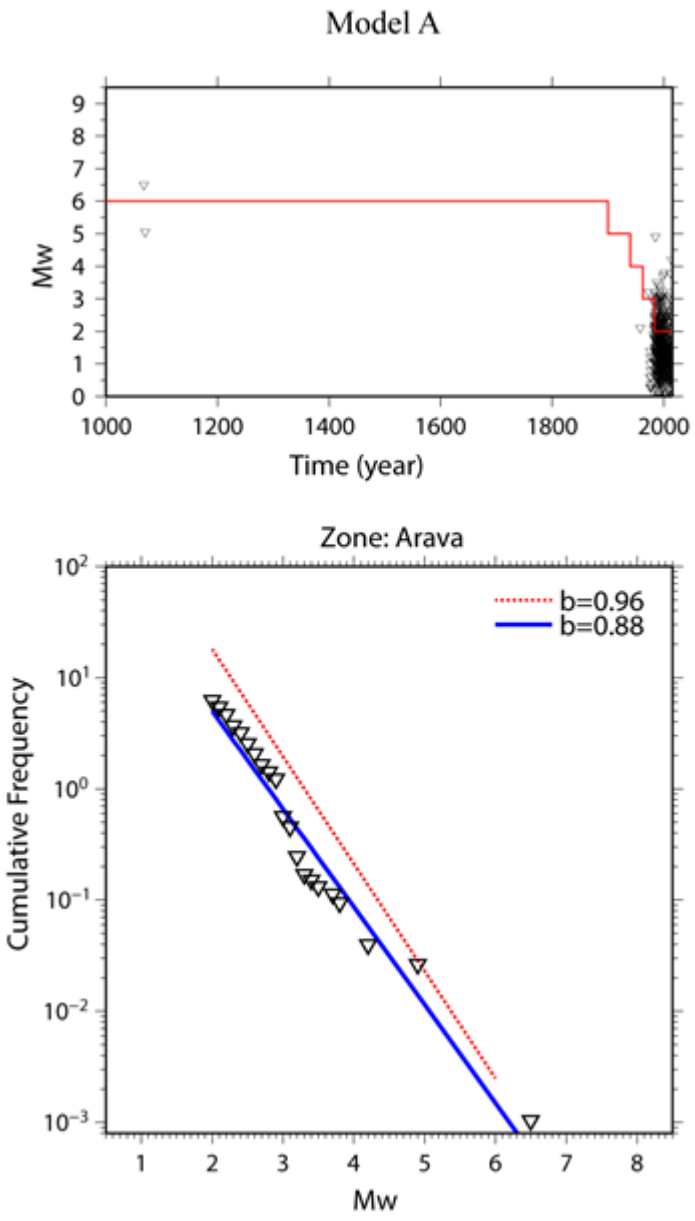

Figure 13. Top panel: model of completeness used in calculations of seismic parameters for Arava seismogenic zone (Model A). Lower panel: Gutenberg – Richter relation for Arava zone. Blue solid line with the slop equal to b-value indicates the best-fit seismicity line. Open triangles show the observed seismicity. Red dotted line models the seismicity for reference value of b=0.96 that is used in Israel Building Code 413.

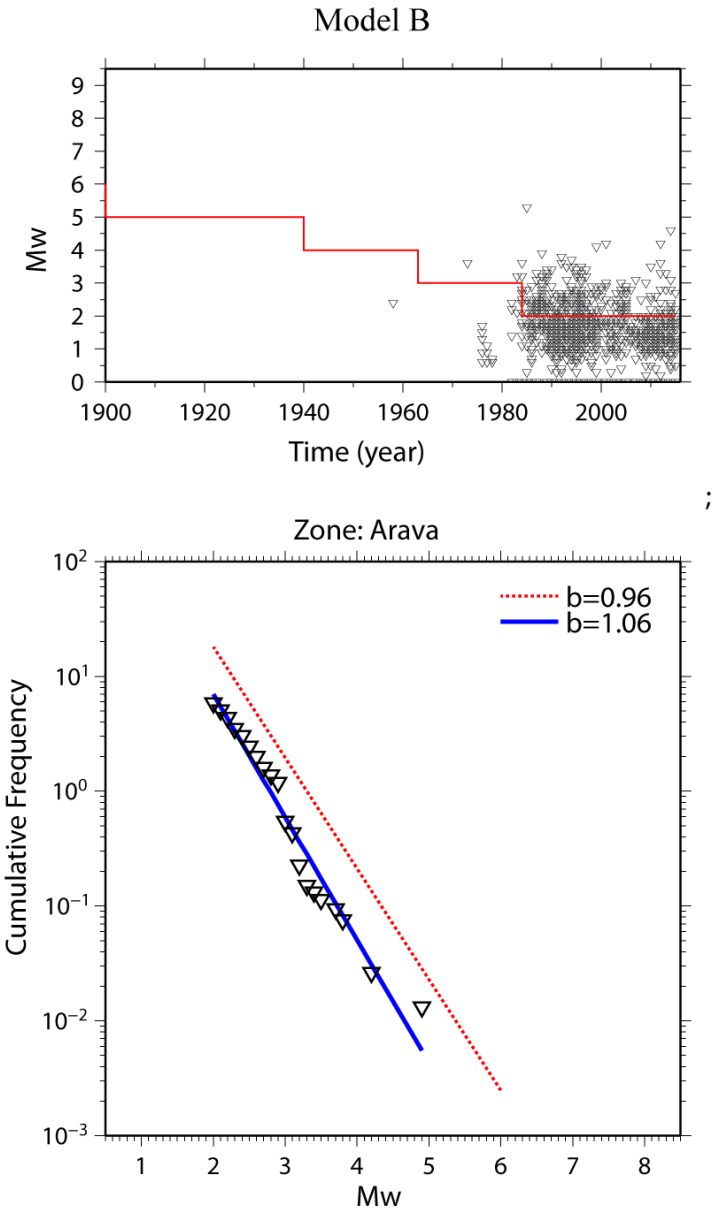

Figure 14. Top panel: model of completeness used in calculations of seismic parameters for seismogenic zone Arava. Lower panel: Gutenberg – Richter relation for Arava zone. Blue solid line with the slop equal to b-value indicates the best-fit seismicity line. Open triangles show the observed seismicity. Red dotted line models the seismicity for reference value of b=0.96 that is used in Israel Building Code 413.

Table 9. Models of completeness for b-value estimation for Arava seismogenic zone.

Model A		**Model B**	
Period	Mw	Period	Mw
1000-1899	6		
1900-1939	5	1900-1939	5
1940-1962	4	1940-1962	4
1963-1985	3	1963-1985	3
1985-2015	2	1985-2015	2
b = 0.88 a = 2.46		b = 1.06 a = 2.79	

Table 10 shows a comparison of observed seismic moment rate and fault slip rate estimated from magnitudes of regional earthquakes that occurred in Arava seismogenic zone with seismic moment rate and slip rate for this area based on recurrence parameters. The comparison is done for two estimated b-value and reference b-value that is used in Israel building code. In the table the row corresponding to reference b-value is marked by gray color.

Table 10. Comparison of seismic moment rate and fault slip rate estimated from observed magnitudes of regional earthquakes and from recurrence parameters obtained for Arava seimogenic area

Fault width, (km)	**a value (Mw min=2)**	**b-value**	**Mo rate observed (N*m/y)**	**Mo rate (N*m/y) Estimated**	**slip rate (mm/y) based on Mo observed**	**slip rate (mm/y) based on recurrence relation**
15	2.3	0.96	1.346E+16	4.07E+15	0.175	0.053
5	2.79	1.06		3.32E+15	0.526	0.130
10					0.263	0.065
15					0.175	0.043
25					0.105	0.026
5	2.46	0.88		2.05E+16	0.526	0.805
10					0.263	0.402
15					0.175	0.268
25					0.105	0.161

As can be seen from the table a fault width has considerable influence and cause a large uncertainty on the slip rate estimate. Based on comparison of observed and estimated seismic moment and slip rate it can be conclude that model A yielding b=0.88 and fault width of W=15 km are in a good agreement with observed seismicity in Arava zone.

6. Hula – Kineret seismogenic zone

Hula-Kineret seismogenic zone is the area in which the DST changes its direction to the northeast so that its strike is not parallel with the overall direction of relative plate motion. In this area a large number of earthquakes occur including two earthquake-producing fault step zones between the Qiryat Shemona, Hula basin and the Kineret basin (Heimann, 1990). To the north of the Hula depression large strike-slip faults are displayed with clear compressional features. The high seismicity in this area appears to delineate parts of the main faults, in particular immediately north of the Sea of Galilee. The earthquakes are characterized by very low magnitudes, and most of them display shallow hypocentral depths above 12 km deep. Length of Hula - Kineret zone that we use in calculations is 80 km.

Previous investigations of the seismicity along segments of the DST reveal that the microearthquakes in the Lake Kinneret basin have a tendency to cluster in space (van Eck and Hofstetter 1990). Previous estimates of b-value in this area fluctuate between 0.8 and 0.86 (Ben-Menahem 1981, 1991; Shapira and Feldman 1987) which is lower than the regional b-value. An interesting observation was made by Kafri and Shapira (1990), who suggested that the activity in the Kinneret region might be related to the water level of the lake and rainfalls. A correlation between the occurrences of felt earthquakes and both the beginning of the rainy season and the annual minimum water level was found. This correlation was explained as a process in which frictional strength along the boundary faults of the Dead Sea fault is reduced by upward flows, triggering an earthquake that would have occurred later due to the tectonic stress.

Table 11 lists the input completeness models for estimation of b-value in Hula – Kineret zone. The last row in the table marked by gray color shows the resulting estimates of a and b-values. Models A and B use large historical events. Model C contains data from instrumental catalog only.

Table 11. Models of completeness for b-value estimation for Hula-Kineret seismogenic zone.

Model A		Model B		Model C	
Period	Mw	Period	Mw	Period	Mw
1200-1899	6	1800-1899	6		
1900-1939	5	1900-1939	5	1900-1939	5
1940-1962	4	1940-1962	4	1940-1962	4
1963-1985	3	1963-1985	3	1963-1985	3
1985-2015	2	1985-2015	2	1985-2015	2
b = 0.76 a = 2.3		b = 0.71 a = 2.12		b = 1.2 a = 2.69	

The b-value calculated for the model C is significantly higher than for the model A and B. (Table 11, Figures 15-17). It seems that b-value might be poorly constrained by model C (Figure 17) because of small range of magnitudes in the analyzed period. It is always desirable that a catalog covers a large span of magnitudes, at least of three magnitude units. It is possible, that Model C covers too short time period to yield an accurate b-value.

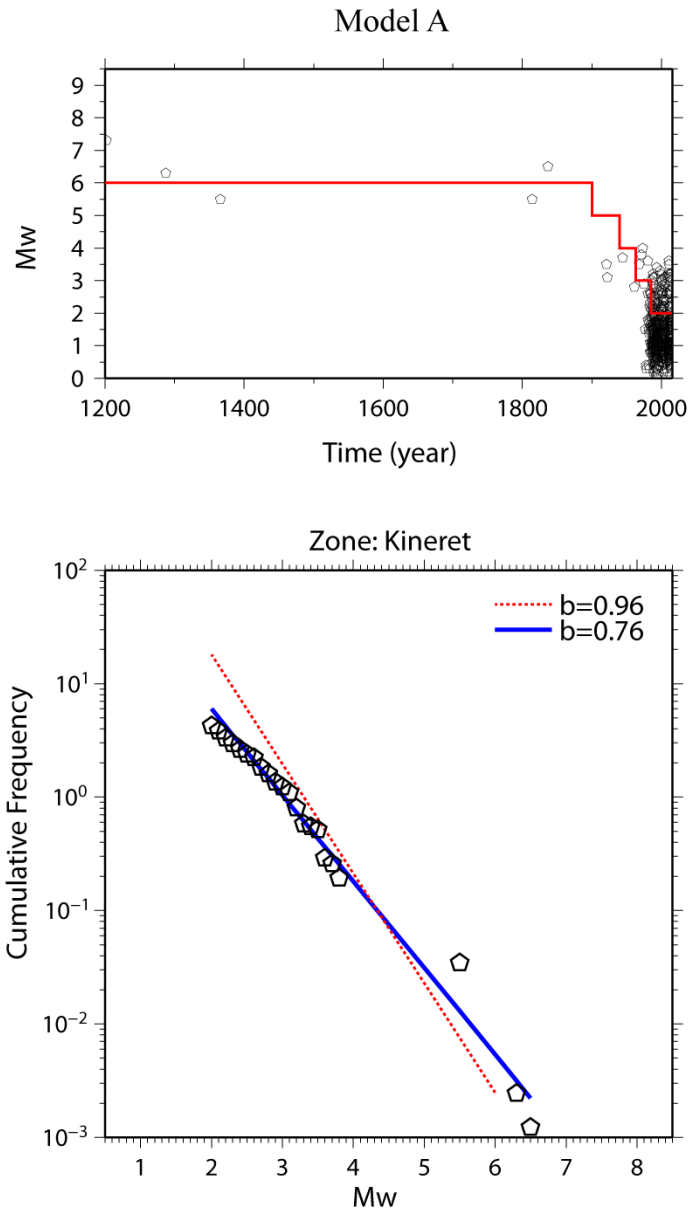

Figure 15. Top panel: model of completeness used in calculations of seismic parameters for Hula – Kineret seismogenic zone (model A). Lower panel: Gutenberg – Richter relation for Hula – Kineret zone. Blue solid line with the slop equal to b-value indicates the modeled seismicity line. Open pentagons show the observed seismicity. Red dotted line models the seismicity for reference value of b=0.96.

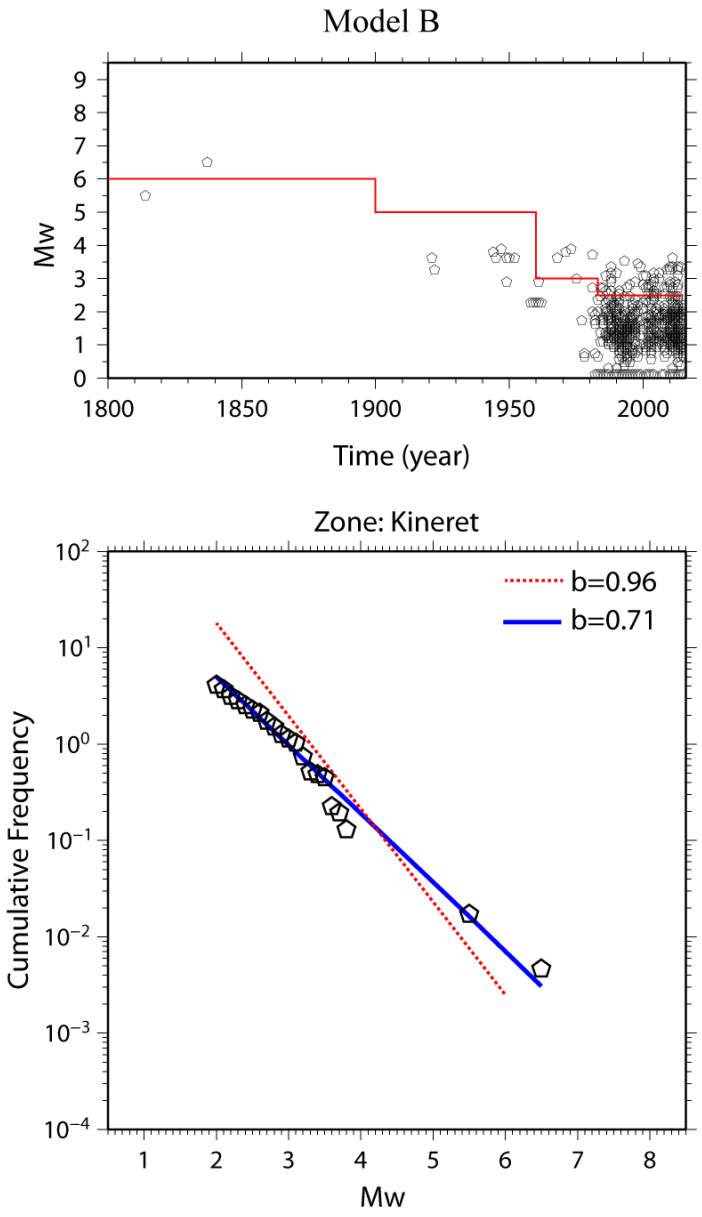

Figure 16. Top panel: model of completeness used in calculations of seismic parameters for Hula – Kineret seismogenic zone (model B). Lower panel: Gutenberg – Richter relation for Hula – Kineret zone. Blue solid line with the slop equal to b-value indicates the modeled seismicity line. Open pentagons show the observed seismicity. Red dotted line models the seismicity for reference value of b=0.96.

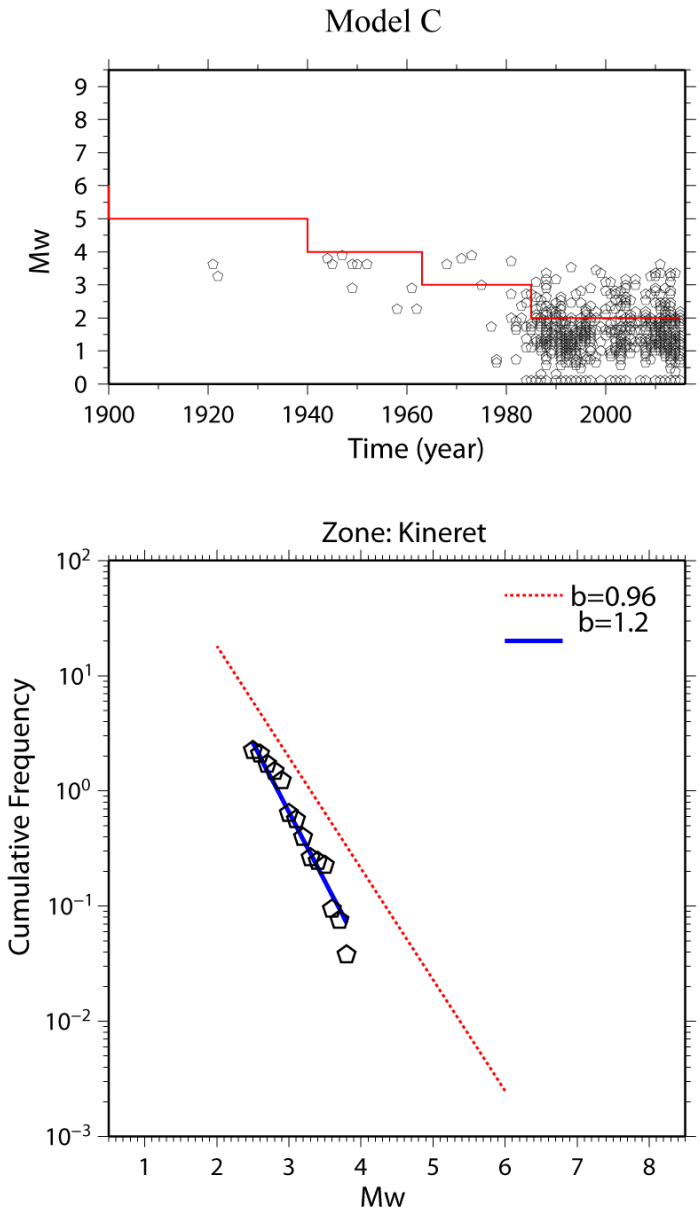

Figure 17. Top panel: model of completeness used in calculations of seismic parameters for Hula – Kineret seismogenic zone (model C) . Lower panel: Gutenberg – Richter relation for Hula – Kineret zone. Blue solid line with the slop equal to b-value indicates the modeled seismicity line. Open pentagons show the observed seismicity. Red dotted line models the seismicity for reference value of b=0.96

Table 12 shows comparison of observed seismic moment and fault slip rates obtained by summing individual seismic moments of events from Hula-Kineret seismogenic zone with seismic moment and fault slip rate for this area calculated as the integral over magnitude of the magnitude-frequency of occurrence data. The row with reference seismic parameters used in Israel for PSHA is marked by gray color. From the comparison of observed and estimated seismic moment rates it is obvious that Model C with resulting a=2.79 and b=1.2 fits well the present-day observed seismicity in Hula-Kineret seismogenic zone. Thought model C yields a reasonable well b-value for small earthquakes it cannot be used for accurate count of larger events.

Table 12. Seismic moment and fault slip rate estimated from observed magnitudes of regional earthquakes and from recurrence parameters obtained for Hula- Kineret seimogenic zone

Fault width, (km)	a value	b-value	Mo rate observed (N*m/y)	Mo rate (N*m/y) Estimated	slip rate (mm/y) based on Mo observed	slip rate (mm/y) based on recurrence relation
15	2.3	0.96	1.01E+14	4.47E+15	0.003	0.12
5	2.79	1.2		3.91E+14	0.008	0.03
10					0.004	0.02
15					0.003	0.01
25					0.002	0.01
5	2.3	0.76			0.008	6.80
10				8.158E+16	0.004	3.40
15					0.003	2.27
25					0.002	1.36
5	2.12	0.71			0.008	9.32
10				1.12E+17	0.004	4.66
15					0.003	3.11
25					0.002	1.86

7. Summary and conclusions

We have applied a and b – value calculations to the whole Israel region and for three specific seismogenic zones by using a maximum-likelihood approach (Wiechert, 1983). The recurrence parameters are obtained with data sets of variable completeness with time. For the purposes of this study we converted catalog's duration magnitudes to the moment magnitudes. As a result, the best-fit estimate of regional b-value that based on instrumental GII catalog is equal to 0.93 that is consistent with the current regional seismicity model. This estimate of regional b-value is slightly lower than the b-values suggested by Shapira and Hofstetter (2002).

The regional b-value estimated by using models of completeness including the historical catalog compiled by GII up to 1200 year decreases to 0.78.

Plots of the cumulative frequency versus magnitude for Dead Sea, Arava and Hula-Kineret regions are given in Figures 9-17. The best fit estimates of b-value for three selected seismogenic zones are varying between 0.76 and 1.2, similar with other areas with strike-slip faults in the world. In general, the b-values are lower than the b-values suggested by Shapira and Hofstetter (2002). The regional a-value concerned with regional seismicity level is estimated as 3.38-3.88 depending on the model of completeness and historical catalog. The a-value concerned with seismogenic zones from Arava to Hula-Kineret changes from 2.1 to 2.8.

The regional maximal magnitude, earthquake rate, and recurrence time are examined as a function of average fault slip rate for several choices of b-value. The moment and slip rate analysis based on estimated in this study magnitude-frequency relations are applied to specific fault areas, i.e., fault length, width and depth extent. Since the slip rates are inversely proportional to the fault width, the constrained parameters are estimated for several values of fault width. The slip rates are estimated by setting fault width to 5 km, 10 km, 15 km and 25 km.

Our analysis indicates that M_{max} defined by Shapira and Hofstetter (2002) for DST region can be underestimated, especially for long periods. Table 3 and Figure 7 demonstrate that for slip rate of 5 mm/y the M_{max} could vary from 7.55 to 8.41. This result is compatible with the assumption of Garfunkel et al. (1981) about the possibility of very strong earthquake (M8-8.5) that could have occurred in the DST in last 4000 y. The existence in the past of even one such strong earthquake is explaining the apparent unusually low seismic efficiency of DST. It is shown that fault width has considerable influence on the M_{max} value. Knowledge of fault width can considerably reduce the uncertainty in M_{max} estimates.

When comparing the rate at which the regional earthquakes occur with that accepted by the plate rates it has been observed to be too small. This result agrees with previous studies (Gargunkel et al., 1981; Salamon et al, 2003; Hofstetter and al., 2013) and supports the conclusion that much motion in analyzed region does not take place on the earthquake faults. Perhaps the missing displacement occurs on creeping faults as continuous deformation.

Comparison of the observed and calculated from recurrence relations seismic moments and fault slip rates can be useful in order to select the appropriate recurrence model for PSHA. When comparing the observed slip rate (obtained from the observed magnitudes of regional earthquakes) with slip rate that is based on the regional seismic model (b = 0.96) for Dead Sea and Arava seismogenic zones the observed slip rate is higher. This observation shows that currently used a and b-values do not agree with present-day regional seismic activity in the selected regions and can yield underestimated seismic hazard. For Hula-Kineret area the observed slip rate is less than predicted by the seismicity model with b=0.96. In the same time the observed slip rate reasonably fits to updated seismicity model with b=1.2.

Based on our analysis and the reviewed literature about evaluation of models of seismicity we found no approach that is fully satisfying for Israel region. Our analysis shows that using the overall constant b-value, as done in many parts of the USA is not appropriate for the Israel region as we show for the Dead Sea and Arava seismogenic zones. From the moment and slip rate analysis it is obvious that current seismic model accepted for National Building Code would yield conservative and even underestimated seismic hazard. The question of when

a regional b-value versus local ones should be used has to be answered directly during the evaluation of seismic parameters.

8. The technique for practical evaluation of regional seismicity model

From this study we can conclude that a further revision to the model of regional seismicity in Israel region including the definition and characterization of seismic source zones should be applied on the basis of new available information: seismological, geological, geophysical and historical. Below we propose the technique for practical evaluation of regional seismicity model.

1. Prior to the maximum likelihood analysis some general questions should be considered. Before b-value could be computed with MLE it should be decided for all zones in which way all the b- values will be computed.

1.1 The most obvious issue is the number, size and configuration of seismogenic zones. It is obvious, that a choice of the zoning model has a significant impact on the resulting hazard. The question is whether the regional seismicity has such a strong stationarity that small zones are necessary to represent a pattern of localized seismicity. The model of 27 seismogenic zones might be considered to be over-detailed, and much simpler zonation could be proposed (which would have the advantage that each larger zone would have more earthquakes to analyze and determine recurrence rates). This question can be raised with respect to the seismicity of zones 3, 5, 12 and 15. Also, it should be mentioned that the regional source model does not completely cover the area of Israel. Some parts of Israel have not been included in the model. Considering aforementioned notes and updated distribution of regional earthquakes we propose the example for model of seismic sources in Israel and adjacent areas, (Figure 18). The final zonation should be based on expert opinion.

1.2 The suitability of b-value or the seismic source zone should be reviewed if the b- value is determined. With respect to seismic hazard our analysis indicates that different approaches should be taken to evaluate seismic hazard depending on type of seismicity that is associated with the analyzed area. Wesnousky and Scholz (1983), for instance, claimed that single faults might not obey the Gutenberg-Richter relation. If data does not support the Gutenberg-Richter earthquake frequency distribution (background seismicity), other models of seismicity should be selected.

1.3 The regions selected must contain sufficient seismicity data for the statistics to be significant, and sub-catalogs corresponding to seismogenic zones should be generated. The b-value parameter is very sensitive to the sample size. It is clear that when there are few events in a zone, the b-value will be poorly constrained or indeterminable. Experience shows that around 100 events are needed to obtain good b-value estimates. Time span of the catalog must be at least comparable and possibly larger than the return period of the largest expected event

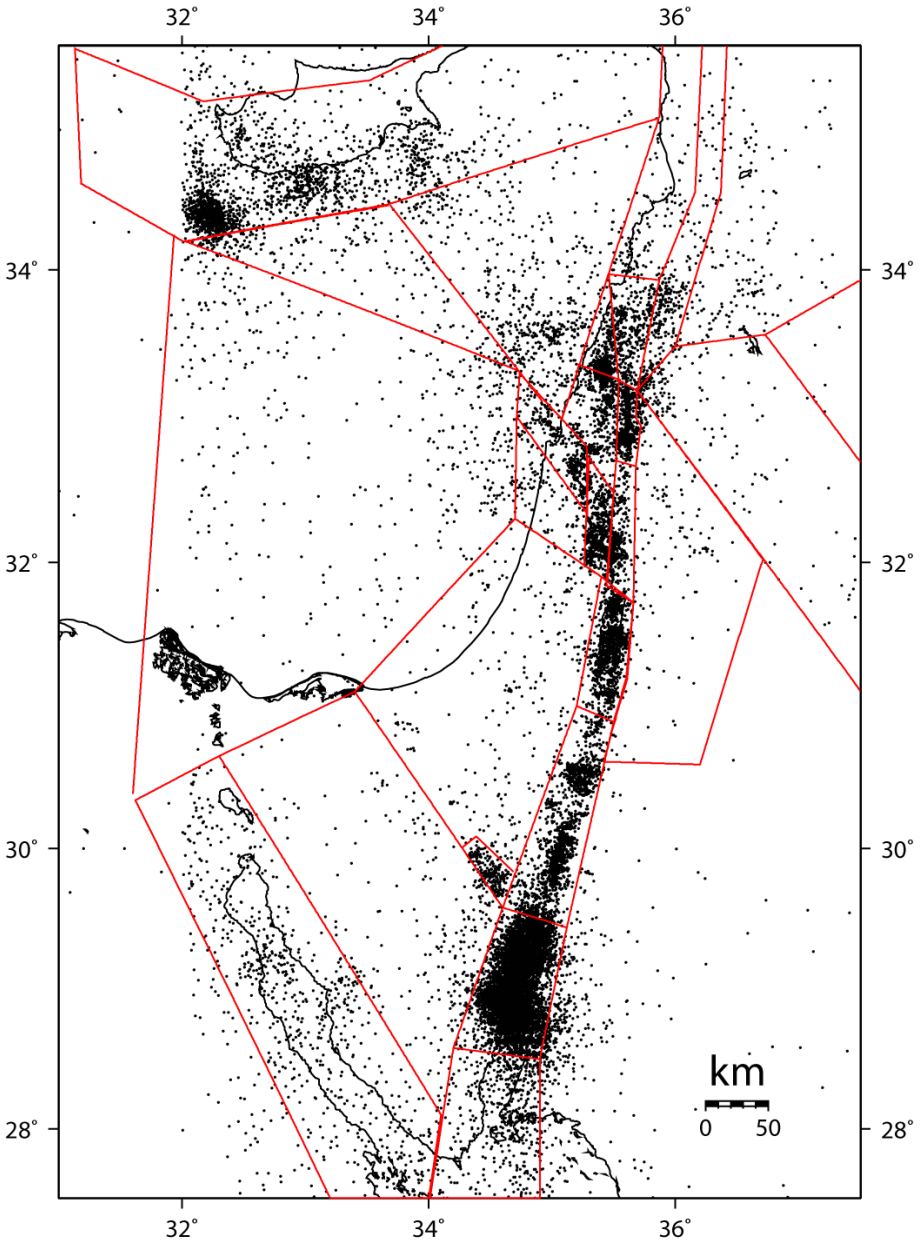

Figure 18. Regional source model proposed in the study.

1.4 Uniform magnitudes for selected sub-catalogs must be available. It is important that reported magnitudes are homogeneous throughout the time period. A span of three or more magnitude units is usually required.

1.5 To avoid dependent data, the catalog has to be de-clustered

1.6 The choice of the magnitude of completeness model quite often influences the result.

1.7 Temporal data stability or stationarity of a and b-value should be analyzed. Original data are separated into several sub-sets for different time periods and evaluated separately. Change in activity rate causes a systematic bias towards a lower b-value. (This arises questions: Will the seismicity of the future follow the pattern of the past? Will areas

which were active in the last centuries remain active also in the next 50–100 years? Or have areas of past seismicity now exhausted their potential and will remain quiet while other areas will become more active?). If we assume that the rate at which earthquakes occur in any increment of magnitude is constant in time, we can combine data gathered over varying durations.

2. Maximum-likelihood estimation (MLE) of b-value in accordance with the chosen of source zoning model, model of completeness and temporal distribution model.

3. A logic tree needs to be developed by experts to account for the uncertainty in the input parameters and to understand the resulting b-value uncertainty. Evaluation of b-value uncertainty is important because small changes in b-value produce large changes in projected numbers of major earthquakes. One way to estimate the uncertainty in the resulting parameters is to propagate the errors associated with all input parameters through the equations. Estimating cumulative error for parameters for which there is considerable uncertainty, such as the completeness of the earthquake record, magnitude, slip rate or fault length and width, is not a simple problem. An alternative method to account for the uncertainty in the estimated parameters, commonly used in seismic hazard models, is the logic tree approach. This method involves selecting a range of reasonable values for each parameter, assigning likelihood to each value. The resulting solution is the median value for every possible combination values plus minus the standard deviation. The lower and upper estimates are the median values plus or minus the standard deviation.

References

Abercrombie, R., E. and Brune, J., N., 1994. Evidence for a constant b-value above magnitude 0 in the southern San Andreas, San Jacinto and San Miguel Fault Zones, and at the Long Valley Caldera, California. Geophysical Research Letters, 21, 1647-1650.

Allen, C.R., Amand, P., Richter, C. F., and Nordquist, J.M., 1965. Relationship between seismicity and geologic structure in the southern California region: Seismol. Soc. America Bull., 55, 753-797.

Amiran D. H., Arieh E. and Turcotte, A., 1994. Eartquakes in Israel and adjacent areas: Maroseismic observations since 100 B.C.E., J. Israel Explaration.

Anderson J., G , 1979. Estimating the seismicity from geological structure for seismic-risk studies. BSSA, 69, 139-158.

Anderson J., G. and J., E., Luco, 1983. Consequences of slip rate constraints on earthquake occurrence relations, BSSA, 2, 471 – 496.

Arieh E. 1967. Seismicity of Israel and adjacent areas. Geol Surv Isr, Bull 43,1–14.

Bayrak Y, and Yılmaztürk A., 2002. Lateral variations of the modal (a/b) values for the different regions of the world, J. Geodynamics, 106.

Ben-Avraham, Z., 1985. Structural framework of the Gulf Elat (Aqaba), northern Red sea. J. Geophys. Res., 90, 703-726.

Ben-Avraham, Z. and G. Schubert, 2006. Deep "Drop Down" Basin in the Southern Dead Sea, Earth Planet. Sci. Lett., 251, 254-263.

Ben-Menahem A, Aboodi E 1971. Tectonic patterns in the Red Sea region, J Geophys Res 76, 2674–2689.

Ben-Menahem, A., 1979. Earthquake Catalogue for the Middle East (92 B.C.-1980 A.D.), Bollettino di Geofisica Teorica ed Applicata, 21, 84, 245-310.

Brune, J.N. 1968. Seismic moment, seismicity, and slip rate along major fault zones, J. Geophys. Res. 73, 777-784.

Gardner, J. K. and Knopoff L. , 1974. Is the sequence of earthquakes in Southern California, with aftershocks removed, Poissonian?, Bull. Seismol. Soc. Am., v. 64, p. 1363-1367.

Garfunkel, Z., Zak, I., and Freund, R., 1981, Active faulting in the Dead Rift: Tectonophysics, v. 80, p. 1–26.

Garfunkel, Z. and Ben-Avraham, Z., 1996. The structure of the Dead Sea basin. Tectonophysics, 266, 155-176.

Ginat, H., Enzel, Y., Avni, Y., 1998. Translocated plio-pleistocene drainage systems along the Arava fault of the Dead Sea Transform, Tectonophysics 284 (1–2), 151–160.

Gvirtzman, Z. and Zaslavsky, Y., 2009. Map of zones with potentially high ground motion amplification: Explanatory notes. (In Hebrew). Isr. Geol. Surv., Rep. GSI/15/2009.

Gutenberg B. and Richter, C. F., 1944. Frequency of Earthquakes in California, Bulletin of the Seismological Society of America, 34, 1944, 185-188.

Hanks, T. C. and Kanamori, H., 1979. A moment magnitude scale, J. Geoph. Res., 84, 2348-2350.

Hamiel, Y., Amit, R., Begin, Z. B., Marco, S., Katz, O, Salamon, A., Zilberman, E. and Porat, N., 2009. The seismicity along the Dead Sea Fault during the last 60,000 years, BSSA, 3, 2020-2026.

Hatzidimitriou, P.M., Papadimitrou, E.E., Mountrakis, D.M., Papazachos, B.C., 1985. The seismic parameter b of the frequency-magnitude relation and its association with geological zones in the area of Greece. Tectonophysics 120,

141–151.The seismic parameter b of the frequency-magnitude relation and its association with the geological zones in the area of Greece

Hofstetter, R. and Ataev G., 2011. Re-examination of correlation coefficients of earthquake source parameter. GII report 556/638/11.

Hofstetter A, Dorbath C, and Calo, M., 2012. Crustal structure of the Dead Sea basin from local earthquake tomography, Geophys. J. Int. 189:554–568.

Hofstetter, A., Dorbath, C., Dorbath, L., 2013. Instrumental data on the seismic activity along the Dead Sea Transform. In: *Dead Sea Transform Fault System: Reviews*. (Z. Garfunkel, Z. Ben-Avraham, E. Kagan, eds.), Springer-Verlag, ISBN 978-94-017-8871-7

Imoto, M., 1991. Changes in the magnitude-frequency b-value prior to large (M=6.0) earthquakes in Japan. Tectonophysics, 193, 311-325.

Kagan, Y., Y., 1991. Seismic moment distribution, Geophys. J. Int., 106, 123-134.

Kagan, Y., Y., 1994. Seismic moment-frequency relation for shallow earthquakes: regional comparison, J. Geophys. Res. 02, 2835-2852.

Klinger, Y., Avouac, J., Dorbath, L., Karaki, N.A., Tisnerat, N., 2000. Seismic behaviour of the Dead Sea fault along Araba valley, Jordan. Geophys. J. Int. 142, 769–782.

Jaumé, S.C., Sykes, L.R., 1999. Evolving towards a Critical Point: A Review of Accelerating Moment/energy Release prior to Large and Great Earthquakes. Pure and Applied Geophysics, 155, 279-306.

Le Beon, M., Y. Klinger, A. Q. Amrat, A. Agnon, L. Dorbath, G. Baer, J.-C. Ruegg, O. Charade, and O. Mayyas, 2008. Slip rate and locking-depth from GPS profiles across the southern Dead Sea Transform, J. Geophys. Res. 113.

Lomnitz-Adler J. and Lomnitz C., 1979. A modified form of the Gutenberg-Richter magnitude-frequency relation, BSSA, 69, 1209–1214.

Main, I., G. and P., W., Burton, 1984. Information theory and the earthquake frequency-magnitude distribution, BSSA, 74, 1409- 1426.

Main, I., G., Meredith, P. G., Jones, C., 1989. A reinterpretation of the precursory seismic b-value anomaly from fracture mechanics. Geoph. J. Int., 96, 131-138.

Manakou M. V and Tsapanos M., 2000. Seismicity and seismic hazard parameters evaluation in the island of Crete and the surrounding area inferred from mixed data files. Tectonophysics, 321, 157–178.

Nuannin, P., Kulhanek, O. and Persson, L., 2005. Spatial and temporal b value anomalies preceding the devastating off coast of NW Sumatra earthquake of December 26, 2004. Geophysical Research Letter, 32, L1130

Pacheco, S., F., Scholz, C., H. and Sykes, L., R., 1992. Changes in frequency-size relationship from small to large earthquakes, Nature, 355, 71- 73.

Popandopoulos and Chatziioannou, 2014. Gutenberg-Richter law parameters analysis using the Hellenic unified seismic network data through Fast Bee technique, Earth Sc., 3, 122-131.

Roy, S., Ghosh, U., Hazra, S., Kayal, J., R., 2012. Fractal Dimension and b value mapping before and after the 2004 megathrust earthquake in the Andaman-Sumatra subduction zone, Extreme Events and Natural Hazards: The complexity perspective,. Washington, D.C., American Geophysical Union, 196, 55-62.

Salamon, A., Hofstetter A., Garfunkel Z. and Ron H. 1996. Seismicity of the eastern Mediterranean region: Perspective from the Sinai subplate. Tectonophysics, 263, 293-305.

Salamon, A., Hofstetter A., Garfunkel Z. and Ron H., 2003. Seismotectonics of the Sinai subplate–the eastern Mediterranean region. Geophys J Int., 155 (1): 149-173.

Sadeh, M., Hamiel, Y., Ziv, A., Bock, Y., Fang, P., Wdowinski, A., 2012. Crustal deformation along the Dead Sea Transform and the Carmel Fault inferred from 12 years of GPS measurements. J. Geophys. Res. 117

Shamir, G., Bartov, Y., Sneh, A., Fleisher, L ., Arad, V. and Rosensaft, M., 2001. Preliminary seismic zonation in Israel, GSI Report No. GSI/12/2001.

Shapira A, Feldman L. 1987. Microseismicity of three locations along the Jordan rift, Tectonophysics 141:89–94.

Shapira A, Hofstetter A., 1993. Source parameters and scaling relationships of earthquakes in Israel, Tectonophysics 217:217–226

Shapira, A. and Hofstetter, A., 2002. Seismicity parameters of seismogenic zones. http://www.seis.mni.gov.il/heb/Teken/seismicity-rprt.htm

Shapira, A. and Hofstetter, R. Abdallah, A., F., Dabbeek, J. and Hays W., 2007. Earthquake hazard assessments for building codes. http://www.lloydthomas.org/5-SpecialStudies/IsraelEarthquakeReport.pdf

Tsapanos T., 1990. b-Values of two tectonic parts in the circum-pacific belt. Pure and appl. Geoph.134, 229–242.

Utsu, T., 1966. A statistical significance test of the difference in b-value between two earthquake groups, J. Phys. Earth 14, 37--40.

Wang, J. H., 1988. b values of shallow earthquakes in Taiwan. Bull. Seism. Soc. Am. 78 (3), 1243–1254.

Wesnousky, S. G., 1986. Earthquakes, Quaternary faults, and seismic hazard in California, J. Geophys. Res. 91, 12587–126731.

Wiemer, S. and Wyss, M., 1997. Mapping the frequency-magnitude distribution in asperities: An improved technique to calculate recurrence times?, J. Geophys. Res., 102,15115-15128.

Weichert, D., H., 1980. Estimation of the earthquake recurrence parameters for unequal observation periods for different magnitudes. Bulletin of the Seismological Society of America 70, 1337-1346.

Wyss, M., 1973. Towards a physical understanding of the earthquake frequency distribution, Geoph. J. R. astr. Soc., 31, 341-359.

Zohar M., Salamon, A. and Rubin, R., 2016. Reappraised list of historical earthquakes that affected Israel and its close surroundings, J Seismology, DOI 10.1007/s10950-016-9575-7.

Yılmazturk, A., Bayrak, Y. and Cakır, O., 1999. Crustal seismicity in and around Turkey. Natural Hazards 18, 253–267.

Youngs R. and Coppersmith K., 1985. Implications of fault slip rates and earthquake recurrence models to probabilistic seismic hazard estimates, BSSA, 75, 939-964.